6 Sun N, Panetta NJ, Gupta DM et al. Feeder-free derivation of induced pluripotent stem cells from adult human adipose stem cells. Proc Natl Acad Sci USA 2009;106:15720–15725.
7 Aasen T, Raya A, Barrero MJ et al. Efficient and rapid generation of induced pluripotent stem cells from human keratinocytes. Nat Biotechnol 2008;26:1276–1284.
8 Loh YH, Agarwal S, Park IH et al. Generation of induced pluripotent stem cells from human blood. Blood 2009;113:5476–5479.
9 Seki T, Yuasa S, Oda M et al. Generation of induced pluripotent stem cells from human terminally differentiated circulating T cells. Cell Stem Cell 2010;7:11–14.
10 Yu J, Hu K, Smuga-Otto K et al. Human induced pluripotent stem cells free of vector and transgene sequences. Science 2009;324: 797–801.
11 Yu J, Chau KF, Vodyanik MA et al. Efficient feeder-free episomal reprogramming with small molecules. PLoS One 2011;6:e17557.
12 Chou BK, Mali P, Huang X et al. Efficient human iPS cell derivation by a non-integrating plasmid from blood cells with unique epigenetic and gene expression signatures. Cell Res 2011;21:518–529.
13 Okita K, Matsumura Y, Sato Y et al. A more efficient method to generate integration-free human iPS cells. Nat Methods 2011;8:409–412.
14 McMahon AP, Bradley A. The Wnt-1 (int-1) proto-oncogene is required for development of a large region of the mouse brain. Cell 1990;62:1073–1085.
15 Fujioka T, Yasuchika K, Nakamura Y et al. A simple and efficient cryopreservation method for primate embryonic stem cells. Int J Dev Biol 2004;48:1149–1154.
16 Niwa H, Yamamura K, Miyazaki J. Efficient selection for high-expression transfectants with a novel eukaryotic vector. Gene 1991; 108:193–199.
17 Mack AA, Kroboth S, Rajesh D et al. Generation of induced pluripotent stem cells from CD34+ cells across blood drawn from multiple donors with non-integrating episomal vectors. PLoS One 2011;6: e27956.
18 Loh YH, Hartung O, Li H et al. Reprogramming of T cells from human peripheral blood. Cell Stem Cell 2010;7:15–19.
19 DePristo MA, Banks E, Poplin R et al. A framework for variation discovery and genotyping using next-generation DNA sequencing data. Nat Genet 2011;43:491–498.
20 Ye Z, Zhan H, Mali P et al. Human-induced pluripotent stem cells from blood cells of healthy donors and patients with acquired blood disorders. Blood 2009;114:5473–5480.
21 Ohgushi M, Matsumura M, Eiraku M et al. Molecular pathway and cell state responsible for dissociation-induced apoptosis in human pluripotent stem cells. Cell Stem Cell 2010;7:225–239.
22 Park IH, Zhao R, West JA et al. Reprogramming of human somatic cells to pluripotency with defined factors. Nature 2008;451:141–146.
23 Tsubooka N, Ichisaka T, Okita K et al. Roles of Sall4 in the generation of pluripotent stem cells from blastocysts and fibroblasts. Genes Cells 2009;14:683–694.
24 Feng B, Jiang J, Kraus P et al. Reprogramming of fibroblasts into induced pluripotent stem cells with orphan nuclear receptor Esrrb. Nat Cell Biol 2009;11:197–203.
25 Han J, Yuan P, Yang H et al. Tbx3 improves the germ-line competency of induced pluripotent stem cells. Nature 2010;463:1096–1100.
26 Maekawa M, Yamaguchi K, Nakamura T et al. Direct reprogramming of somatic cells is promoted by maternal transcription factor Glis1. Nature 2011;474:225–229.
27 Marson A, Foreman R, Chevalier B et al. Wnt signaling promotes reprogramming of somatic cells to pluripotency. Cell Stem Cell 2008; 3:132–135.
28 Edel MJ, Menchon C, Menendez S et al. Rem2 GTPase maintains survival of human embryonic stem cells as well as enhancing reprogramming by regulating p53 and cyclin D1. Genes Dev 2010;24:561–573.
29 Zhao Y, Yin X, Qin H et al. Two supporting factors greatly improve the efficiency of human iPSC generation. Cell Stem Cell 2008;3: 475–479.
30 Mali P, Ye Z, Hommond HH et al. Improved efficiency and pace of generating induced pluripotent stem cells from human adult and fetal fibroblasts. Stem Cells 2008;26:1998–2005.
31 Subramanyam D, Lamouille S, Judson RL et al. Multiple targets of miR-302 and miR-372 promote reprogramming of human fibroblasts to induced pluripotent stem cells. Nat Biotechnol 2011;29:443–448.
32 Peterson C, Legerski R. High-frequency transformation of human repair-deficient cell lines by an Epstein-Barr virus-based cDNA expression vector. Gene 1991;107:279–284.
33 Gore A, Li Z, Fung HL et al. Somatic coding mutations in human induced pluripotent stem cells. Nature 2011;471:63–67.
34 Serwold T, Hochedlinger K, Inlay MA et al. Early TCR expression and aberrant T cell development in mice with endogenous prerearranged T cell receptor genes. J Immunol 2007;179:928–938.
35 Trickett A, Kwan YL. T cell stimulation and expansion using anti-CD3/CD28 beads. J Immunol Methods 2003;275:251–255.
36 Hanna J, Saha K, Pando B et al. Direct cell reprogramming is a stochastic process amenable to acceleration. Nature 2009;462:595–601.
37 Saridakis V, Sheng Y, Sarkari F et al. Structure of the p53 binding domain of HAUSP/USP7 bound to Epstein-Barr nuclear antigen 1 implications for EBV-mediated immortalization. Mol Cell 2005;18: 25–36.
38 Li M, Chen D, Shiloh A et al. Deubiquitination of p53 by HAUSP is an important pathway for p53 stabilization. Nature 2002;416:648–653.
39 Staerk J, Dawlaty MM, Gao Q et al. Reprogramming of human peripheral blood cells to induced pluripotent stem cells. Cell Stem Cell 2010;7:20–24.

See www.StemCells.com for supporting information available online.

Hindawi Publishing Corporation
BioMed Research International
Volume 2013, Article ID 134813, 10 pages
http://dx.doi.org/10.1155/2013/134813

Hindawi

Research Article

An Active C-Terminally Truncated Form of Ca^{2+}/Calmodulin-Dependent Protein Kinase Phosphatase-N (CaMKP-N/PPM1E)

Atsuhiko Ishida,[1] Kumiko Tsumura,[1] Megu Oue,[1] Yasuhiro Takenaka,[2] Yasushi Shigeri,[2] Naoki Goshima,[2] Yasuhiro Ishihara,[1] Tetsuo Hirano,[1] Hiromi Baba,[3] Noriyuki Sueyoshi,[3] Isamu Kameshita,[3] and Takeshi Yamazaki[1]

[1] *Laboratory of Molecular Brain Science, Graduate School of Integrated Arts and Sciences, Hiroshima University, Higashi-Hiroshima 739-8521, Japan*
[2] *National Institute of Advanced Industrial Science and Technology, Ikeda, Osaka 563-8577, Japan*
[3] *Department of Life Sciences, Faculty of Agriculture, Kagawa University, Kagawa 761-0795, Japan*

Correspondence should be addressed to Atsuhiko Ishida; aishida@hiroshima-u.ac.jp

Received 5 April 2013; Revised 10 July 2013; Accepted 12 July 2013

Academic Editor: Y. George Zheng

Ca^{2+}/calmodulin-dependent protein kinase phosphatase (CaMKP/PPM1F) and its nuclear homolog CaMKP-N (PPM1E) are Ser/Thr protein phosphatases that belong to the PPM family. CaMKP-N is expressed in the brain and undergoes proteolytic processing to yield a C-terminally truncated form. The physiological significance of this processing, however, is not fully understood. Using a wheat-embryo cell-free protein expression system, we prepared human CaMKP-N (hCaMKP-N(WT)) and the truncated form, hCaMKP-N(1–559), to compare their enzymatic properties using a phosphopeptide substrate. The hCaMKP-N(1–559) exhibited a much higher V_{max} value than the hCaMKP-N(WT) did, suggesting that the processing may be a regulatory mechanism to generate a more active species. The active form, hCaMKP-N(1–559), showed Mn^{2+} or Mg^{2+}-dependent phosphatase activity with a strong preference for phospho-Thr residues and was severely inhibited by NaF, but not by okadaic acid, calyculin A, or 1-amino-8-naphthol-2,4-disulfonic acid, a specific inhibitor of CaMKP. It could bind to postsynaptic density and dephosphorylate the autophosphorylated Ca^{2+}/calmodulin-dependent protein kinase II. Furthermore, it was inactivated by H_2O_2 treatment, and the inactivation was completely reversed by treatment with DTT, implying that this process is reversibly regulated by oxidation/reduction. The truncated CaMKP-N may play an important physiological role in neuronal cells.

1. Introduction

Ca^{2+}/calmodulin-dependent protein kinase phosphatase (CaMKP/PPM1F/POPX2) was first identified in rat brain as a unique protein phosphatase that specifically dephosphorylates and regulates multifunctional CaMKs, including CaMKI, II, and IV [1–4]. Thereafter, another protein phosphatase with 52% identity in the catalytic domain to human CaMKP was found in the human cDNA databases (Figure 1(a)). When the cDNA was expressed in COS cells, the phosphatase encoded by the cDNA was localized to the nucleus, in contrast to CaMKP, which was exclusively found in the cytosol. Therefore, we named the enzyme CaMKP-N for its localization in the nucleus [5]. Subsequently, other groups named this enzyme POPX1 [6] or PPM1E [7] and reported that it is involved in the negative regulation of the p21-activated protein kinase [6] and the 5′-AMP-activated protein kinase [7]. Gene knockdown experiments for zebrafish CaMKP-N (zCaMKP-N) using morpholino-based antisense oligonucleotides indicated that CaMKP-N is essential for the early development of the brain and spinal cord in zebrafish [8].

We also showed that the proteolytic processing of zCaMKP-N plays a critical role in the regulation of its catalytic activity, subcellular localization, and substrate targeting [9]. In accordance with these results, Kitani et al.

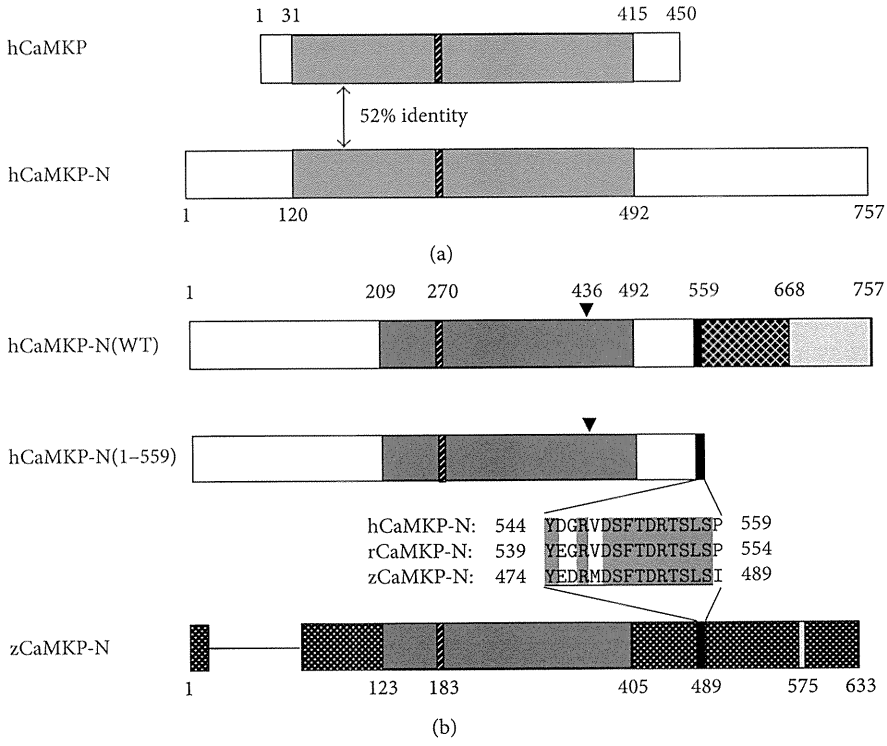

FIGURE 1: Schematic representation of hCaMKP, hCaMKP-N(WT), hCaMKP-N(1–559), and zCaMKP-N. (a) Comparison of the primary structure of hCaMKP-N with that of hCaMKP. The regions that show significant homology are shown in grey. (b) Domain structures of hCaMKP-N(WT), hCaMKP-N(1–559), and z-CaMKP-N. Catalytic domains are shown in dark grey, and the hatched bars within them indicate the PP2C motif that is characteristic of PPM family phosphatases. Black bars show the antibody recognition site. In hCaMKP-N, the recognition site is located just to the N-terminal side of the putative processing site. The amino acid sequences of the antibody recognition site in human, rat, and zebrafish CaMKP-N are also indicated. Underline shows the amino acid sequence used for generating the anti-CaMKP-N antibody. Closed arrowheads show the position of Cys436, which may be responsible for redox regulation of the phosphatase activity (see text). It has been reported that two nuclear localization signals are located in the region that is C-terminal side to Arg668 on hCaMKP-N (shown in light grey). The 575–587 region of zCaMKP-N reportedly functions as a nuclear localization signal (shown in light grey) [8]. The amino acid residue numbers of the respective phosphatases are also shown.

[10] suggested that the majority of CaMKP-N undergoes proteolytic processing to generate a 90 kDa fragment in rat brain that is localized to the cytosol. Since the amino acid sequence homology between zCaMKP-N and human CaMKP-N (hCaMKP-N) is only 48% and the molecular size of zCaMKP-N is much smaller than the size of hCaMKP-N (by more than 100 amino acid residues, Figure 1(b)), it is difficult to predict, on the basis of sequence homology, whether the 90 kDa fragment is a mammalian counterpart for the active fragment of zCaMKP-N that is generated by proteolytic processing in zebrafish. It is clinically significant to explore the enzymatic properties of hCaMKP-N, which may provide a molecular basis for drug development because CaMKP-N has been suggested to regulate the 5′-AMP-activated protein kinase involved in the pathogenesis of diabetes [7]. Unfortunately, difficulty in preparing hCaMKP-N in a sufficient purity and quantity has hampered the biochemical characterization of this enzyme. Our initial attempt to obtain pure full-length hCaMKP-N using transfected Sf9 cells failed due to proteolysis during the expression and purification. We performed only a preliminary characterization of hCaMKP-N using a mixed preparation that contained both full-length hCaMKP-N and its truncated fragment, which was generated during the preparation [5]. Therefore, no information has been available about the enzymatic properties and the physiological importance of each species of hCaMKP-N.

In this study, we utilized a wheat-embryo cell-free protein expression system to separately prepare full-length hCaMKP-N and hCaMKP-N(1–559), a human counterpart to the 90 kDa truncated fragment found in the rat brain. Using these preparations, we compared the kinetic properties of full-length hCaMKP-N and the truncated fragment, and we found that the truncated fragment had much higher phosphatase activity than the full-length form. We also examined the enzymatic properties of the truncated hCaMKP-N, which had not been characterized in detail, and discussed the physiological importance of the processing.

2. Materials and Methods

2.1. Materials. The phosphopeptides, pp2 (MHRQE**T(p)**VDC), pp4 (MHRQE**S(p)**VDC), pp6 (MHRQE**Y(p)**VDC), and pp10 (YGGMHRQE**T(p)**VDC), were synthesized using a Shimadzu PSSM-8 automated peptide synthesizer and

purified by reverse-phase HPLC on a C_{18} column [5, 11]. The identity and purity of the peptides were confirmed by time-of-flight mass spectrometry. The postsynaptic density (PSD) fraction was purified from rat cerebral cortex as described by Sahyoun et al. [12]. The anti-CaMKP-N antibody was obtained as previously described [8]. Monoclonal anti-CaMKIIα (MAb CBα-2) was purchased from Life Technologies. The anti-active CaMKII was from Promega. The biotin-conjugated rabbit anti-mouse IgG was obtained from ZYMED. The anti-rabbit Ig, biotinylated species-specific antibody, streptavidin-conjugated horseradish peroxidase, and the Ni^{2+}-Sepharose high-performance resin were from GE Healthcare. An enhanced chemiluminescence detection agent, SuperSignal West Femto Maximum Sensitivity Substrate, was from Thermo Scientific. DNase-free RNase was from Boeringer Mannheim. Hydrogen peroxide, Quick CBB, and okadaic acid were purchased from Wako Pure Chemical Industries, and the 1-amino-8-naphthol-2,4-disulfonic acid (ANDS) was from Tokyo Chemical Industry. Calyculin A was from Millipore/Upstate. All other agents were obtained from Nacalai Tesque or Sigma-Aldrich.

2.2. Construction of Plasmids. The pEU-E01-CaMKPN vector, which encodes the wild type (WT) hCaMKP-N with an N-terminal 6x His tag, was prepared as described in the following. The following primers were used for PCR: CaMKPN His-UP1 (5′-GGA TAT CTA TGT CGT ACT ACC ATC ACC ATC ACC ATC ACG CCG GCT GCA TCC CTG AGG AGA A-3′) with an *EcoR*V site (underlined) and CaMKPN LP1 (5′-GGT CGA CTT ATT CTA TTT TAT AGC TCC AAG GAA GAT-3′) with a *Sal*I site (underlined). The PCR was performed in a PTC-200 Thermal Cycler (MJ Research) for 20 cycles, each consisting of denaturation for 5 s at 98°C, annealing for 30 s at 60°C, and extension for 2 min at 68°C, in the presence of 3% (v/v) dimethyl sulfoxide using Pyrobest DNA Polymerase (Takara) and the plasmid DNA containing hCaMKP-N cDNA (AK289966, HuPEX clone FLJ76651) as the template. After gel purification, the amplified product was digested with *EcoR*V and *Sal*I and cloned into pCR4Blunt-TOPO (Invitrogen). The plasmid DNA was then sequenced with the ABI PRISM 3100 Genetic Analyzer (Applied Biosystems) to confirm the DNA sequence of the cloned insert. The plasmid was digested with *EcoR*V and *Sal*I, and the insert purified by gel purification was ligated into pEU-E01-MCS (CellFree Science) at the *EcoR*V and *Sal*I sites to generate pEU-E01-CaMKPN, which encodes the full-length hCaMKP-N with an N-terminal 6× His-tag. The pEU-E01-CaMKPN(1–559) vector, which encodes the C-terminal deletion mutant hCaMKP-N(1–559) with an N-terminal 6× His tag, was prepared using an inverse PCR mutagenesis kit (KOD-Plus-Mutagenesis Kit, TOYOBO) according to the manufacturer's instructions, with pEU-E01-CaMKPN as the template. The PCR was performed in a PC707 Thermal Cycler (ASTEC) for 10 cycles, each consisting of denaturation for 10 s at 98°C, annealing for 30 s at 60°C, and extension for 6 min at 68°C, in the presence of 4.8% (v/v) dimethyl sulfoxide with the sense primer (5′-TAG ATC CCA AAT CAA CGT GCT GGA AGA C-3′, underline shows the site of mutation) and the antisense primer (5′-TGG GCT CAG GCT AGT TCT ATC AGT G-3′). The PCR product was digested with *Dpn*I, and after gel purification, the amplified product was phosphorylated and self-ligated to generate pEU-E01-CaMKPN(1–559). The sequence of the mutated insert was confirmed by DNA sequencing.

2.3. The Cell-Free Expression of Recombinant hCaMKP-Ns and Its Purification. Cell-free expression of hCaMKP-N(WT) and hCaMKP-N(1–559) was carried out using a wheat-embryo cell-free protein expression system, the WEPRO 1240H Expression Kit (CellFree Sciences), according to the manufacturer's instruction, with either pEU-E01-CaMKPN or pEU-E01-CaMKPN(1–559). The *in vitro* translation reactions were conducted in a 96-well microtiter plate at 15°C for 18–20 hs. After the translation reaction, DNase-free RNase (24 μg/mL) and the cOmplete Mini EDTA-free protease inhibitor cocktail (Roche) (1 tablet/10 mL) were added to the translation reaction mixture, and the mixture was incubated for 30 min on ice. To 3 mL of the mixture, 0.96 mL of 50% (v/v) suspension of Ni^{2+}-Sepharose resin, which had been equilibrated and suspended in 20 mM Tris-HCl (pH 7.5) containing 0.2% (v/v) Tween 40, 10 mM imidazole, 300 mM NaCl, and 1 mM DTT, was added, and the mixture was then gently rocked at 4°C for 1 h. All of the following purification procedures were carried out at 4°C. The gel slurry was poured into an empty column (0.12 × 14 cm), and the flow-through fraction was allowed to drain. The column was washed with 5 mL of 20 mM Tris-HCl (pH 7.5) containing 0.05% (v/v) Tween 40, 20 mM imidazole, 1.5 M NaCl, and 1 mM DTT. For CaMKP-N(WT), the column was further washed with 2.5 mL of 20 mM Tris-HCl (pH 7.5) containing 0.05% (v/v) Tween 40, 100 mM imidazole, 300 mM NaCl, and 1 mM DTT, or for CaMKP-N(1–559), the column was further washed with 20 mM Tris-HCl (pH 7.5) containing 0.05% (v/v) Tween 40, 40 mM imidazole, 300 mM NaCl, and 1 mM DTT. The column was eluted with 2.5 mL of 20 mM Tris-HCl (pH 7.5) containing 0.05% (v/v) Tween 40, 250 mM imidazole, 300 mM NaCl, and 1 mM DTT, and the eluate was concentrated using a centrifugal filter unit (10,000 MWCO, Millipore). Glycerol was added to a final concentration of 30% (v/v). The purified enzymes were aliquoted and could be stored at −80°C for several months without any detectable loss in activity.

2.4. Protein Phosphatase Assays. Protein phosphatase assays using a phosphopeptide as a substrate were performed as previously described [13]. The phosphopeptides used in this study were derived from the amino acid sequence around the Thr286 autophosphorylation site on CaMKIIα (CaMKII(281–289) = pp2) or its analogs (pp4, pp6, pp10). The reaction was initiated by adding enzyme, and the reaction mixture was incubated at 30°C for 45 min. The amount of inorganic phosphate released in the mixture during the incubation was determined by malachite green assay [11]. The Michaelis-Menten kinetic parameters were determined from a direct fit to the Michaelis-Menten equation using a nonlinear regression program (DeltaGraph, version 6.0,

Red Rock Software) as previously described [11]. The tested compounds were added to the reaction systems mentioned above at the indicated concentrations.

The protein phosphatase assay using autophosphorylated CaMKII as a phosphoprotein substrate was performed as described [13] with the following modifications. The PSD fraction (905 μg/mL) was incubated at 5°C for 10 min in the reaction mixture (100 μL) containing 40 mM Hepes-NaOH (pH 8.0), 5 mM $Mg(CH_3COO)_2$, 0.1 mM EGTA, 1 μM calmodulin, 0.8 mM $CaCl_2$, 0.01% Tween 20, and 50 μM nonradioactive ATP to autophosphorylate the CaMKII found in the PSD fraction. After the reaction, the mixture was immediately diluted with 1 mL of ice-cold wash buffer consisting of 50 mM Tris-HCl (pH 7.5), 0.2 M NaCl, 0.05% Tween 40, 0.1 μM calyculin A, and 0.1 mM DTT, and then it was centrifuged for 10 min at 4°C in a microcentrifuge at maximum speed. The supernatant was removed, and the precipitate was resuspended with the ice-cold wash buffer and centrifuged again as described previously. The washing procedure was repeated five more times. The precipitate obtained was resuspended in 100 μL of the washing buffer and stored at −80°C until it was used. The phosphatase reaction was carried out in a reaction mixture containing 50 mM Tris-HCl (pH 7.5), 2 mM $MnCl_2$, 0.1 mM EGTA, and 0.01% Tween 20. Western blotting analysis using anti-active CaMKII (anti-PCaMKII, 1 : 1000 dilution) was performed to estimate the extent of autophosphorylation at the Thr286 site on CaMKII. After the detection of autophosphorylated CaMKII, the blot was treated with Blot Restorte Membrane Rejuvenation Kit (Millipore) according to the manufacturer's instructions, so that it could be reprobed. To confirm the amount of total CaMKII on the blot, the rejuvenated blot was reprobed with a monoclonal anti-CaMKIIα (CBα-2, 1 : 500 dilution).

2.5. Binding of hCaMKP-N(1–559) to PSD. hCaMKP-N(1–559) (1 μg) was incubated with the PSD fraction (1 μg) in 50 mM Tris-HCl (pH 7.5) (10 μL) on ice for 1 h and then centrifuged for 5 min at 4°C in a microcentrifuge at maximum speed. The pellet fraction was suspended with ice-cold 50 mM Tris-HCl (pH 8.1) containing 0.85% NaCl (1 mL), and the suspension was centrifuged as described previously. The washing procedure was repeated, and the pellet fraction was resuspended in a minimum volume of 50 mM Tris-HCl (pH 8.1) containing 0.85% NaCl. An equal volume of 2× SDS-sample buffer was added to the suspension to prepare the samples for western blotting analysis.

2.6. Western Blotting Analysis. The protein samples were separated by gel electrophoresis and transferred onto an Immobilon-P polyvinylidene difluoride membrane (Millipore) as previously described [14]. After blocking, the membrane was incubated overnight at 4°C with primary antibodies and then incubated with the biotinylated rabbit anti-mouse IgG (1 : 2000 dilution) or anti-rabbit Ig biotinylated species-specific antibody (1 : 2000 dilution) for 2 h at room temperature. This step was followed by incubation with a streptavidin-horseradish peroxidase conjugate (1 : 500 dilution) for 40 min at room temperature. The western blots were visualized by an enhanced chemiluminescence detection procedure using LAS-1000 (GE Healthcare) image analyzers.

2.7. Other Analytical Methods. SDS-PAGE was carried out according to the Laemmli method [15]. Protein concentrations were determined using an advanced protein assay reagent (cytoskeleton) with bovine serum albumin as a standard. The concentrations of the pp2 and pp4 peptides were determined by measuring the Pi released after alkali hydrolysis as previously described [11]. The concentration of the pp6 peptide was determined by measuring the Pi released after acid hydrolysis as previously described [11]. The concentration of the pp10 peptide was determined spectrophotometrically using the absorption coefficient for tyrosine ($\varepsilon_{278} = 1.16 \times 10^3\ M^{-1}\ cm^{-1}$).

3. Results

3.1. Preparation of hCaMKP-N and hCaMKP-N(1–559) Using a Wheat-Embryo Cell-Free Protein Expression System. It has been reported that CaMKP-N undergoes proteolytic processing in the rat brain to generate a 90 kDa fragment in which the C-terminal region is truncated [10]. In an attempt to evaluate the physiological significance of the C-terminal truncation of hCaMKP-N, we prepared full-length and truncated hCaMKP-N to compare their enzymatic properties. Kitani et al. [10] reported that rat CaMKP-N is truncated at or near Pro554. Since the amino acid sequence identity between rat and human CaMKP-N is very high (88%) [16], we constructed expression plasmids for the full-length hCaMKP-N (hCaMKP-N(WT)) and for the truncated hCaMKP-N fragment, in which the C-terminal side of the corresponding Pro residue (Pro559) was deleted, (hCaMKP-N(1–559)), and both contain an added 6× His-tag at their N-terminus (Figure 1(b)). Using the expression plasmids as templates, we synthesized the full-length hCaMKP-N and hCaMKP-N(1–559) proteins with a wheat-embryo cell-free protein expression system and purified these enzymes by Ni^{2+}-Sepharose affinity chromatography as described in Section 2. The purified hCaMKP-N(WT) and hCaMKP-N(1–559) showed apparent molecular masses of approximately 120 kDa and 90 kDa on SDS-PAGE, respectively (Figure 2(a)), which are in good agreement with the previous report [5]. Both enzymes were detected by the anti-CaMKP-N antibody that was raised against a synthetic peptide corresponding to the 474–488 region of zCaMKP-N (Figure 2(b)). Because this region shares fairly high homology with the region that is N-terminal side to Pro559 on hCaMKP-N (Figure 1(b)) [8], it was confirmed that the purified phosphatases retained the N-terminal side of Pro559. It should be noted that the hCaMKP-N(WT) preparation was essentially free from the 90 kDa proteolytic fragment usually seen in the preparations purified from the baculovirus-transfected Sf9 cells [5].

3.2. Activation of hCaMKP-N by C-Terminal Truncation. Using the protein preparations described previously, the

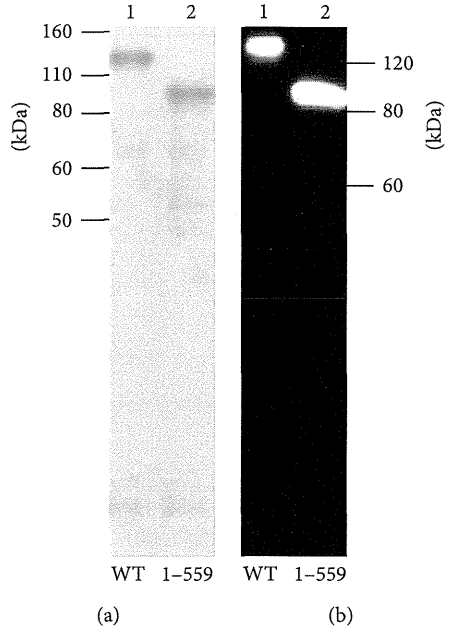

FIGURE 2: hCaMKP-N and its truncation mutant prepared by a wheat-embryo cell-free protein expression system. (a) hCaMKP-N(WT) (lane 1, 2.5 μg) and hCaMKP-N(1–559) (lane 2, 2.5 μg), which had been prepared and purified as described in Section 2, were subjected to SDS-PAGE on a 10% polyacrylamide gel. The gel was stained with Coomassie Brilliant Blue (CBB) using Quick CBB. (b) hCaMKP-N(WT) (lane 1) and hCaMKP-N(1–559) (lane 2) were subjected to SDS-PAGE on a 10% polyacrylamide gel and analyzed by western blotting analysis using an anti-CaMKP-N antibody (1 : 250 dilution) as the primary antibody.

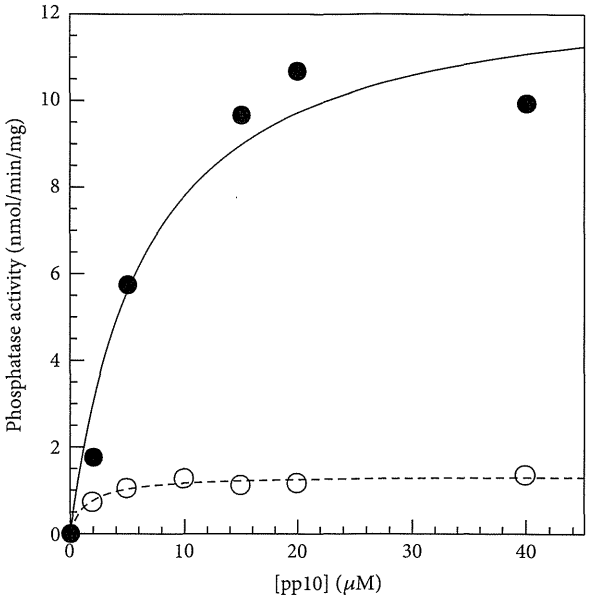

FIGURE 3: Dephosphorylation of a phosphopeptide substrate pp10 by hCaMKP-N(WT) and hCaMKP-N(1–559). The indicated concentrations of pp10 were dephosphorylated by hCaMKP-N(WT) (open circles) and by hCaMKP-N(1–559) (closed circles) at 30°C as described in Section 2. The amount of inorganic phosphate released in the reaction mixture during the reaction was determined as described. The indicated curves were obtained by direct fits of the data to Michaelis-Menten equation. The data shown are those in a representative experiment of at least three independent determinations with similar results.

kinetic properties of hCaMKP-N(WT) and hCaMKP-N(1–559) were evaluated and compared. The phosphatase activities were assessed under the standard assay conditions for CaMKP and CaMKP-N [5, 11], where they were assayed in the presence of 2 mM Mn^{2+} using the pp10 phosphopeptide as a substrate (Figure 3). hCaMKP-N(1–559) showed much higher activity than hCaMKP-N(WT). We performed a kinetic analysis of hCaMKP-N(WT) and hCaMKP-N(1–559) with varying concentrations of the pp10 substrate. They displayed typical Michaelis-Menten kinetics, and the K_m value for pp10 and the V_{max} value were determined (Figure 3, Table 1). These parameters strongly suggested that the truncation of the C-terminal region of hCaMKP-N results in a marked increase in the V_{max} for the phosphatase activity.

3.3. Some Enzymatic Properties of hCaMKP-N(1–559). Since the C-terminally truncated form has been reported to be the most abundant species of CaMKP-N in the rat brain [10], the enzymatic properties of hCaMKP-N(1–559) were further examined using pp10 as the substrate. As shown in Figure 4(a), the truncated fragment showed a strong Mn^{2+}-dependent phosphatase activity and a weak Mg^{2+}-dependent phosphatase activity but no Ca^{2+}-dependent activity. We also examined the effect of varying concentrations of Mn^{2+} and Mg^{2+} on the phosphatase activity (Figure 4(b)). Only a

TABLE 1: Comparison of the phosphatase activities of hCaMKP-N(WT) and hCaMKP-N(1–559). hCaMKP-N(WT) and hCaMKP-N(1–559) were assayed using varying concentrations of the pp10 substrate as described in Section 2. Michaelis-Menten kinetic parameters were determined from a direct fit to the Michaelis-Menten equation. The data represent the average of three independent experiments ± S.D.

	K_m (μM)	V_{max} (nmol/min/mg)
hCaMKP-N(WT)	2.0 ± 0.9	1.4 ± 0.1
hCaMKP-N(1–559)	5.4 ± 0.1	16.3 ± 3.6

submillimolar concentration of Mn^{2+} was required for the full activity of hCaMKP-N(1–559), whereas more than 10 mM Mg^{2+} was required for the same level of activity. A kinetic analysis revealed that the half-maximal activations for Mn^{2+} and Mg^{2+} are 0. 22 ± 0.04 mM and 6.4 ± 1.6 mM, respectively. It should be noted that almost the same level of full activity was observed at their saturating levels, regardless of whether Mn^{2+} or Mg^{2+} was used as a cofactor.

It has been reported that PPM family phosphatases, including PP2C and CaMKP, strongly prefer phospho-Thr over phospho-Ser as the residue to be dephosphorylated [11, 17]. Therefore, we examined the phosphoamino acid residue preference of hCaMKP-N(1–559). For this purpose,

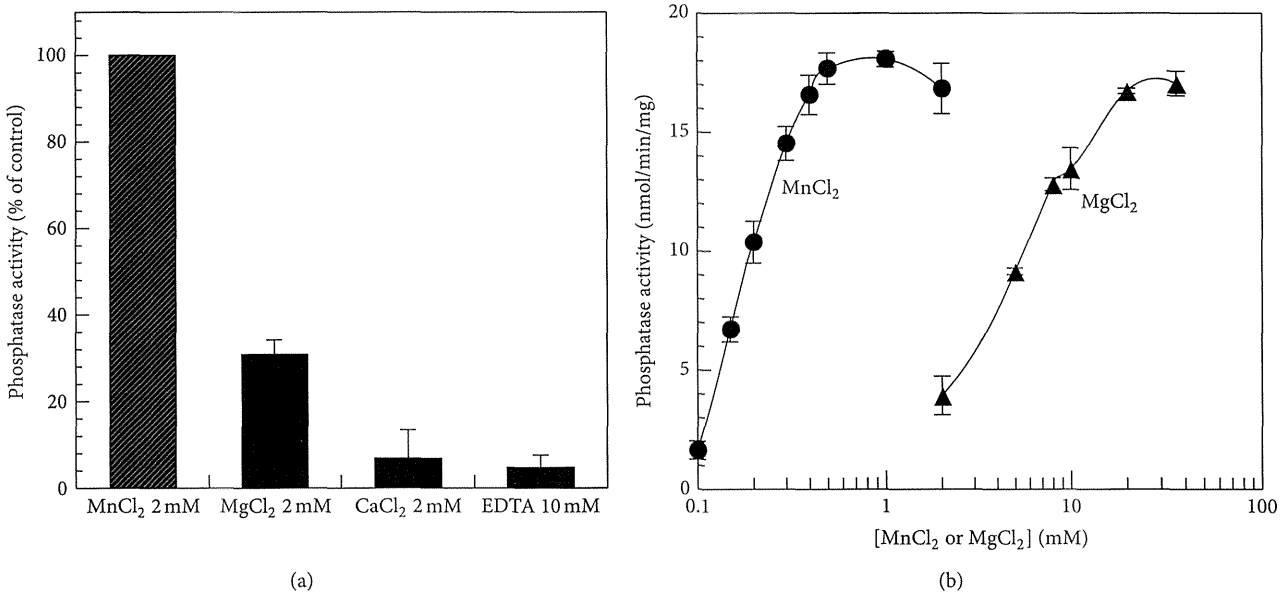

FIGURE 4: The divalent cation requirement for the phosphatase activity of hCaMKP-N(1–559). (a) hCaMKP-N(1–559) was assayed using pp10 as the substrate in the presence of the indicated divalent cations or EDTA instead of 2 mM $MnCl_2$ as described in Section 2. The results are expressed as the percentage of the activity determined with 2 mM $MnCl_2$. The data represent the average of three independent experiments ± S.D. (b) hCaMKP-N(1–559) was assayed using pp10 as the substrate in the presence of varying concentrations of $MnCl_2$ (circles) or $MgCl_2$ (triangles) instead of 2 mM $MnCl_2$.

a synthetic phospho-CaMKII(281–289) peptide (named pp2) and its analogs, in which phospho-Thr was replaced with phospho-Ser (named pp4) or with phospho-Tyr (named pp6), were used as substrates for hCaMKP-N(1–559). The truncated hCaMKP-N efficiently dephosphorylated the parent phospho-Thr peptide pp2, but it barely dephosphorylated the phospho-Ser peptide (pp4) and the phospho-Tyr peptide (pp6), indicating strong preference for phospho-Thr residues as was observed for other PPM family phosphatases (Figure 5).

The effects of some protein phosphatase inhibitors on hCaMKP-N(1–559) were also examined and are shown in Figure 6. Okadaic acid (1 μM) and calyculin A (1 μM), potent PP1 and PP2A inhibitors, had no effect on the phosphatase activity. This is because hCaMKP-N is classified as PPM family phosphatases of which structures are quite different from those of PPP family phosphatases such as PP1 and PP2A. In contrast, NaF (100 mM) and EDTA (10 mM) severely inhibited the phosphatase. It is interesting that ANDS, a CaMKP-specific inhibitor [18], did not inhibit the phosphatase activity of hCaMKP-N(1–559) even at 30 μM, a concentration at which the rat CaMKP was strongly inhibited.

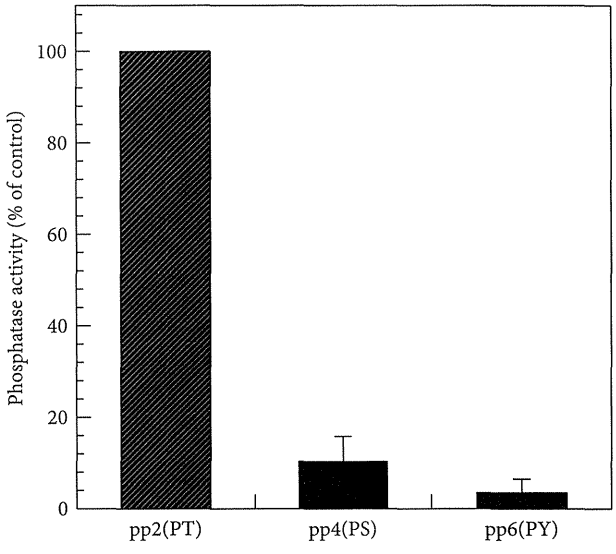

FIGURE 5: The residue preference at the dephosphorylation site. hCaMKP-N(1–559) was assayed using the indicated phosphopeptides (20 μM) as substrates under the standard assay conditions as described in Section 2. The results are expressed as a percentage of the activity determined using pp2 as the substrate. The data represent the average of three independent experiments ± S.D.

3.4. Dephosphorylation of the Autophosphorylated CaMKII in PSD by hCaMKP-N(1–559). CaMKII, one of the candidates for the physiological substrate of hCaMKP-N(1–559), is known to exist abundantly in PSD. Therefore, we examined interaction of hCaMKP-N(1–559) and the rat brain PSD as described in Section 2. The endogenous rat CaMKP-N fragment was not detected in the isolated PSD fraction prepared from the rat brain (Figure 7(a), lane 1). Sequence homology between the rat and human CaMKP-N and the sequence homology between the rat and human CaMKIIα are very high (88% and 99% identity, resp.). After the PSD fraction was incubated with hCaMKP-N(1–559) on ice for 1 h, a significant amount of the CaMKP-N fragment was detected in the PSD fraction (Figure 7(a), lane 2).

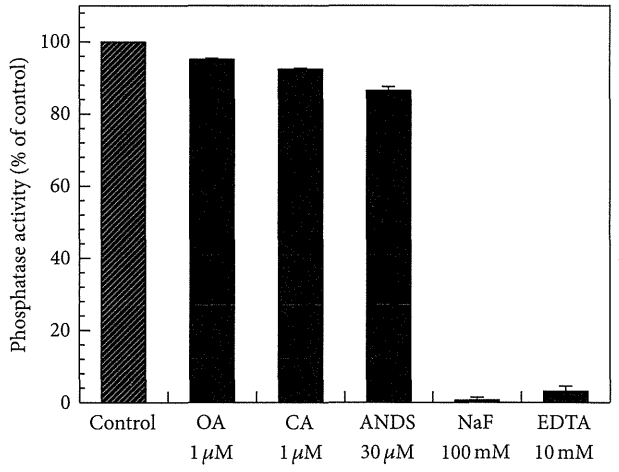

FIGURE 6: The effects of various inhibitors on the phosphatase activity of hCaMKP-N(1–559). hCaMKP-N(1–559) was assayed using pp10 as the substrate in the presence of the indicated compounds. The results are expressed as a percentage of the activity determined with no compound added (control). The abbreviations used in the figure are as follows: OA: okadaic acid; CA: calyculin A; ANDS: 1-amino-8-naphthol-2,4-disulfonic acid. The data represent the average of three independent experiments ± S.D.

Since the PSD-associated CaMKP-N fragment may play a physiological role, the phosphatase activity of hCaMKP-N(1–559) on the autophosphorylated CaMKII was examined. The endogenous CaMKII in the rat PSD fraction was autophosphorylated in the presence of Ca^{2+}/calmodulin and was used as a substrate for hCaMKP-N(1–559). Under the autophosphorylation conditions used, no significant band shift for the CaMKIIα subunit was observed by SDS-PAGE. As shown in Figure 7(b), the autophosphorylated CaMKII was dephosphorylated by hCaMKP-N(1–559) (lane 2). Therefore, hCaMKP-N(1–559) can bind to PSD to dephosphorylate the autophosphorylated CaMKII.

3.5. The Reversible Regulation of hCaMKP-N(1–559) by Oxidation/Reduction. We have reported that incubation of human CaMKP with H_2O_2 leads to the formation of a disulfide bond, which results in inactivation of the enzyme [19]. As shown in Figure 8(a), H_2O_2 also inactivated hCaMKP-N(1–559) in a dose-dependent manner. When the inactivated hCaMKP-N(1–559) was further incubated on ice for 30 min with the reducing agent DTT, the phosphatase activity was restored to almost original levels (Figure 8(b)). This indicates that the inactivation of hCaMKP-N(1–559) by H_2O_2 is a reversible process and that hCaMKP-N(1–559) is reversibly regulated by oxidation/reduction.

4. Discussion

Based on the subcellular localization of transiently expressed hCaMKP-N in COS cells [5], it had been assumed that mammalian CaMKP-N is localized only in the nucleus. However, Kitani et al. [10] showed that in the rat brain, CaMKP-N undergoes proteolytic processing to form a 90 kDa fragment that is localized mainly in the cytosol. Similar proteolytic fragment of CaMKP-N was also found in human frontal cortex [20]. Therefore, the truncated form of hCaMKP-N may have important functions in cells.

In this study, we used a wheat-embryo cell-free protein expression system for preparation of hCaMKP-N and its fragment to minimize proteolysis during the expression and purification of hCaMKP-N. Using this system in conjunction with conventional Ni^{2+}-NTA agarose chromatography, we were able to individually prepare the full-length hCaMKP-N, hCaMKP-N(WT), and its proteolytic fragment, hCaMKP-N(1–559), for the first time without mutual contamination. Typically, approximately 15 μg of purified hCaMKP-N or its fragment could be obtained from 1 well of a translation reaction mixture (21 μL of the wheat-embryo translation mixture and 206 μL of the substrate solution) in a 96-well microtiter plate (data not shown). The wheat-embryo cell-free protein expression system has been proven useful for the preparation of the proteins that are readily degraded by cellular proteases. Because the protease activities detected in the cell-free system are very low [21, 22], this method may be applicable to other protease-sensitive proteins that are difficult to prepare using conventional cell-based expression systems such as Sf9 cells.

Using these preparations, we could rigorously compare the catalytic properties of hCaMKP-N(1–559) and hCaMKP-N(WT). Both hCaMKP-N species have phosphatase activities in the presence of Mn^{2+} toward the pp10 phosphopeptide substrate, which was based on the amino acid sequence around the critical Thr286 autophosphorylation site on CaMKII. This result indicates that the proteolytic fragment is not a degraded and inactive species, but instead, it has phosphatase activity. Although the K_m value for the fragment was somewhat higher than the K_m value for the hCaMKP-N(WT), the V_{max} value for the fragment was more than ten times higher than that for the WT. Therefore, we suggest that the truncation of C-terminal region 560–757 of hCaMKP-N is a post-translational regulatory mechanism to generate a highly active species.

The mechanism of activation by truncation remains unclear. The truncated C-terminal region might act as an autoinhibitory domain, as is the case for calcineurin [23]. Alternatively, processing of the region might cause a conformational change in its catalytic center that leads to catalytic activation. It has been reported that some protein phosphatases in the PPP family are activated by proteolysis [24, 25]. We have also reported that zCaMKP-N is activated by proteolytic processing of the C-terminal domain [9]. Therefore, activation by C-terminal truncation appears to be a common feature for CaMKP-N, despite the fact that hCaMKP-N and zCaMKP-N have fairly different molecular sizes and primary structures. Because it has been reported that rat CaMKP-N(1–554), a fragment corresponding to hCaMKP-N(1–559), is localized in the cytosol of transfected COS cells [10], the truncation of the C-terminal domain is likely to regulate catalytic activity as well as the intracellular localization of hCaMKP-N. Since inhibition of the proteolytic processing of zCaMKP-N in Neuro2a cells by proteasome

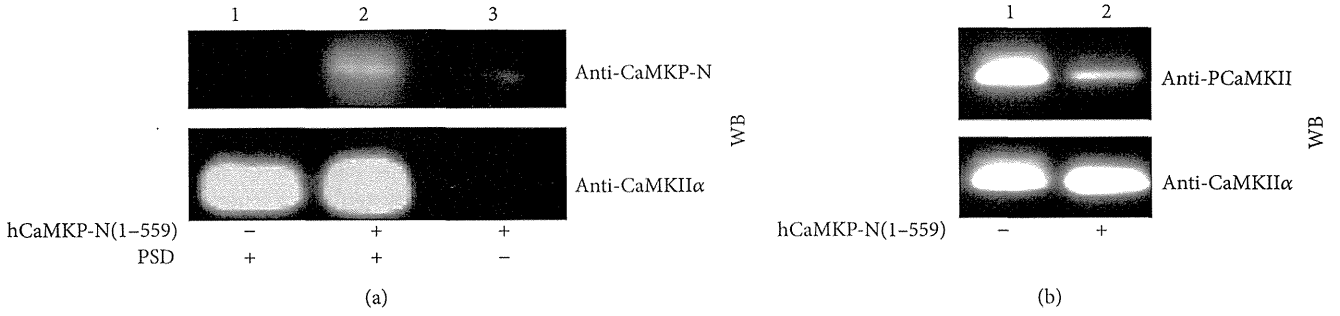

FIGURE 7: The binding of hCaMKP-N(1–559) to PSD and the dephosphorylation of the autophosphorylated CaMKII. (a) hCaMKP-N(1–559) (1 μg) was incubated on ice for 1 h with (lane 2) or without (lane 3) the PSD fraction (1 μg) as described in Section 2. After incubation, the mixture was centrifuged, and the pellet fraction was washed twice with 50 mM Tris-HCl (pH 7.5) containing 0.85% NaCl, followed by western blotting analysis using anti-CaMKP-N antibody (upper panel). Recovery of the PSD fraction was confirmed by probing the same blot using anti-CaMKIIα antibody (lower panel). To check the endogenous CaMKP-N levels, the PSD fraction was also incubated in the absence of hCaMKP-N(1–559) as a control (lane 1). (b) The PSD fraction (29 μg/mL), in which CaMKII had been autophosphorylated as described, was incubated at 30°C with (lane 2) or without (lane 1) hCaMKP-N(1–559). After incubation for 30 min, the phosphatase reaction was terminated by adding excess EDTA (20 mM), and aliquots were analyzed by western blotting to examine the extent of phosphorylation at Thr286 on CaMKII (upper panel, anti-PCaMKII) and the total amount of CaMKIIα on the blot (lower panel, anti-CaMKIIα). The data presented are representative of at least three independent experiments with similar results.

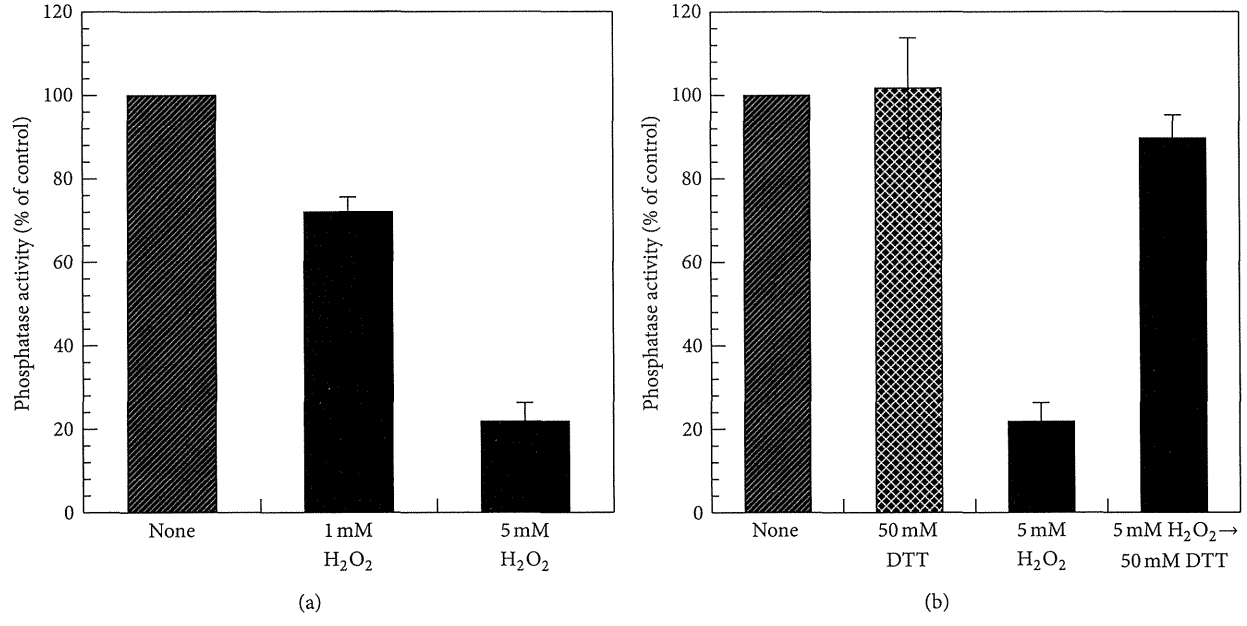

FIGURE 8: The reversible inactivation of hCaMKP-N(1–559) by H_2O_2. (a) hCaMKP-N(1–559) (245 μg/mL) was incubated on ice for 30 min in 25 mM Tris-HCl (pH 7.5) with or without the indicated concentrations of H_2O_2, and then the phosphatase activities were determined using pp10 as the substrate. (b) hCaMKP-N(1–559) (245 μg/mL) was incubated on ice for 30 min in 25 mM Tris-HCl (pH 7.5) with 5 mM H_2O_2, and then DTT (50 mM) was added for incubation on ice for an additional 30 min. Thereafter, the phosphatase activity was determined using pp10 as the substrate. As a comparison, the phosphatase activity without DTT treatment is also presented (5 mM H_2O_2). The DTT treatment itself had no significant effects on the activity of hCaMKP-N(1–559) in the control (50 mM DTT). The results are expressed as a percentage of the control activity (none), which was determined after incubation without any compounds (H_2O_2 or DTT) added. The data represent the average of three independent experiments ± S.D.

inhibitors significantly changed substrate targeting in the cells [9], activation and translocation of the mammalian CaMKP-N may also affect the intracellular substrate targeting.

The activated CaMKP-N fragment generated by the proteolytic processing is reported to be the major species of CaMKP-N in the rat brain [10]. Here, we show a molecular characterization of the 90 kDa active fragment in human, hCaMKP-N(1–559). It exhibited okadaic acid/calyculin A-insensitive and Mn^{2+} or Mg^{2+}-dependent phosphatase activity and demonstrated a striking preference for a phosphothreonyl peptide over a phosphoseryl or a phosphotyrosyl

peptide. These enzymatic properties are similar to those of CaMKP [11]. However, the metal dependence of hCaMKP(1–559) was somewhat different from that of CaMKP. Although the half-maximal activation for Mn^{2+} is comparable to that of rat CaMKP (~0.2 mM), activation by Mg^{2+} is more prominent in hCaMKP(1–559) than it is in CaMKP [26]. Furthermore, hCaMKP-N(1–559) showed Mn^{2+}-dependent activity and comparable Mg^{2+}-dependent activity at its saturating levels. NaF is known to inhibit various protein phosphatases. Fluoride is reported to directly bind to the metal ions in the active center of bovine purple acid phosphatase [27]. Since Ser/Thr protein phosphatases are known to be metalloenzymes that employ dinuclear metal center similar to purple acid phosphatases [28], it is most likely that fluoride also binds to the metal center to inhibit its phosphatase activity. Interestingly, ANDS, a potent inhibitor for CaMKP [18], did not inhibit the phosphatase activity of hCaMKP-N(1–559). This suggests that the three-dimensional structure of the active site of hCaMKP-N is considerably different from that of rat CaMKP even though their primary structures of their putative catalytic regions are highly homologous.

hCaMKP-N(1–559) could bind to PSD to dephosphorylate the CaMKII associated with it. Based on electron microscope results, the corresponding CaMKP-N fragment is suggested to be concentrated in PSD together with CaMKII in rat brain [10]; however, the endogenous rat CaMKP-N fragment was not detected in the isolated PSD fraction. Therefore, it is likely that the CaMKP-N fragment is not a component of PSD, but its binding to PSD is dynamically regulated in neuronal cells. This fragment might be involved in regulation of CaMKII activity in PSD, where synaptic transmission is tightly controlled. The CaMKP-N activated by proteolysis might be a critical regulator for synaptic transmission through controlling the phosphorylation state of the CaMKII in PSD.

Another notable finding in this study is that hCaMKP-N(1–559) is inactivated by H_2O_2 treatment, and reactivated by incubation with DTT. Recently, we reported that human CaMKP is reversibly regulated by oxidation/reduction at Cys359 [19]. This Cys residue is adjacent to an Asp residue that is essential for metal binding at the active site, and the Cys-Asp sequence is conserved in the catalytic sites of many PPM family enzymes including hCaMKP-N. Therefore, the observed inactivation of hCaMKP-N(1–559) might be due to reversible oxidation at Cys436 of hCaMKP-N. The reversible regulation of the phosphatase activity of hCaMKP-N(1–559) by oxidation/reduction may be an important mechanism for regulating the phosphorylation levels of CaMKII in neuronal cells, especially in PSD, in response to oxidative stress.

In summary, we showed for the first time that hCaMKP-N is activated through truncation of the C-terminal domain. The active truncated fragment could bind to PSD to dephosphorylate CaMKII, and its enzymatic properties were similar to those of CaMKP except for its Mg^{2+}-dependence and sensitivity to ANDS. Very recently, genome-wide association studies suggested that single nucleotide polymorphisms found in the loci for CaMKP-N (PPM1E) and for CaMKP (PPM1F) are associated with testicular germ cell tumor [29] and with both schizophrenia and bipolar disorders [30], respectively. Since hCaMKP-N(1–559) is supposedly localized in the cytosol where CaMKP is found, the next important question concerns what are the roles that CaMKP and the active CaMKP-N fragment share in the cytosol. Further work is needed to address this question.

Abbreviations

ANDS: 1-Amino-8-naphthol-2,4-disulfonic acid
CaMKII: Ca^{2+}/calmodulin-dependent protein kinase II
CaMKP: Ca^{2+}/calmodulin-dependent protein kinase phosphatase
hCaMKP-N: Human Ca^{2+}/calmodulin-dependent protein kinase phosphatase-N
PSD: Postsynaptic density
zCaMKP-N: Zebrafish Ca^{2+}/calmodulin-dependent protein kinase phosphatase-N.

Conflict of Interests

The authors reveal that there is no conflict of interests in this paper.

Acknowledgments

This work was supported, in part, by Grants-in-Aid for Scientific Research (21590334) from the Ministry of Education, Science, Sports, and Culture of Japan and by a grant from the Japan Foundation for Applied Enzymology.

References

[1] A. Ishida, I. Kameshita, and H. Fujisawa, "A novel protein phosphatase that dephosphorylates and regulates Ca^{2+}/calmodulin-dependent protein kinase II," *Journal of Biological Chemistry*, vol. 273, no. 4, pp. 1904–1910, 1998.

[2] A. Ishida, S. Okuno, T. Kitani, I. Kameshita, and H. Fujisawa, "Regulation of multifunctional Ca^{2+}/calmodulin-dependent protein kinases by Ca^{2+}/calmodulin-dependent protein kinase phosphatase," *Biochemical and Biophysical Research Communications*, vol. 253, no. 1, pp. 159–163, 1998.

[3] T. Kitani, A. Ishida, S. Okuno, M. Takeuchi, I. Kameshita, and H. Fujisawa, "Molecular cloning of Ca^{2+}/calmodulin-dependent protein kinase phosphatase," *Journal of Biochemistry*, vol. 125, no. 6, pp. 1022–1028, 1999.

[4] A. Ishida, N. Sueyoshi, Y. Shigeri, and I. Kameshita, "Negative regulation of multifunctional Ca^{2+}/calmodulin-dependent protein kinases: physiological and pharmacological significance of protein phosphatases," *British Journal of Pharmacology*, vol. 154, no. 4, pp. 729–740, 2008.

[5] M. Takeuchi, A. Ishida, I. Kameshita, T. Kitani, S. Okuno, and H. Fujisawa, "Identification and characterization of CaMKP-N, nuclear calmodulin-dependent protein kinase phosphatase," *Journal of Biochemistry*, vol. 130, no. 6, pp. 833–840, 2001.

[6] C. Koh, E. Tan, E. Manser, and L. Lim, "The p21-activated kinase PAK is negatively regulated by POPX1 and POPX2, a pair of serine/threonine phosphatases of the PP2C family," *Current Biology*, vol. 12, no. 4, pp. 317–321, 2002.

[7] M. Voss, J. Paterson, I. R. Kelsall et al., "Ppm1E is an in cellulo AMP-activated protein kinase phosphatase," *Cellular Signalling*, vol. 23, no. 1, pp. 114–124, 2011.

[8] T. Nimura, N. Sueyoshi, A. Ishida et al., "Knockdown of nuclear Ca^{2+}/calmodulin-dependent protein kinase phosphatase causes developmental abnormalities in zebrafish," *Archives of Biochemistry and Biophysics*, vol. 457, no. 2, pp. 205–216, 2007.

[9] N. Sueyoshi, T. Nimura, T. Onouchi et al., "Functional processing of nuclear Ca^{2+}/calmodulin-dependent protein kinase phosphatase (CaMKP-N): evidence for a critical role of proteolytic processing in the regulation of its catalytic activity, subcellular localization and substrate targeting in vivo," *Archives of Biochemistry and Biophysics*, vol. 517, no. 1, pp. 43–52, 2012.

[10] T. Kitani, S. Okuno, Y. Nakamura, H. Tokuno, M. Takeuchi, and H. Fujisawa, "Post-translational excision of the carboxyl-terminal segment of CaM kinase phosphatase N and its cytosolic occurrence in the brain," *Journal of Neurochemistry*, vol. 96, no. 2, pp. 374–384, 2006.

[11] A. Ishida, Y. Shigeri, Y. Tatsu et al., "Substrate specificity of Ca^{2+}/calmodulin-dependent protein kinase phosphatase: kinetic studies using synthetic phosphopeptides as model substrates," *Journal of Biochemistry*, vol. 129, no. 5, pp. 745–753, 2001.

[12] N. Sahyoun, H. LeVine III, and D. Bronson, "Cytoskeletal calmodulin-dependent protein kinase. Characterization, solubilization, and purification from rat brain," *Journal of Biological Chemistry*, vol. 260, no. 2, pp. 1230–1237, 1985.

[13] T. Onouchi, N. Sueyoshi, A. Ishida, and I. Kameshita, "Phosphorylation and activation of nuclear Ca^{2+}/calmodulin-dependent protein kinase phosphatase (CaMKP-N/PPM1E) by Ca^{2+}/calmodulin-dependent protein kinase I, (CaMKI)," *Biochemical and Biophysical Research Communication*, vol. 422, no. 4, pp. 703–709, 2012.

[14] E. Harlow and D. Lane D, *Antibodies: A Laboratory Manual*, Cold Spring Harbor Laboratory Press, Cold Spring Harbor, NY, USA, 1988.

[15] U. K. Laemmli, "Cleavage of structural proteins during the assembly of the head of bacteriophage T4," *Nature*, vol. 227, no. 5259, pp. 680–685, 1970.

[16] T. Kitani, S. Okuno, M. Takeuchi, and H. Fujisawa, "Subcellular distributions of rat CaM kinase phosphatase N and other members of the CaM kinase regulatory system," *Journal of Neurochemistry*, vol. 86, no. 1, pp. 77–85, 2003.

[17] A. Donella Deana, C. H. Mac Gowan, P. Cohen, F. Marchiori, H. E. Meyer, and L. A. Pinna, "An investigation of the substrate specificity of protein phosphatase 2C using synthetic peptide substrates; Comparison with protein phosphatase 2A," *Biochimica et Biophysica Acta*, vol. 1051, no. 2, pp. 199–202, 1990.

[18] N. Sueyoshi, T. Takao, T. Nimura et al., "Inhibitors of the Ca^{2+}/calmodulin-dependent protein kinase phosphatase family (CaMKP and CaMKP-N)," *Biochemical and Biophysical Research Communications*, vol. 363, no. 3, pp. 715–721, 2007.

[19] H. Baba, N. Sueyoshi, Y. Shigeri, A. Ishida, and I. Kameshita, "Regulation of Ca^{2+}/calmodulin-dependent protein kinase phosphatase (CaMKP) by oxidation /reduction at Cys-359," *Archives of Biochemistry and Biophysics*, vol. 526, no. 1, pp. 9–15, 2012.

[20] A. L. Jessen, *Characterization of the protein phosphatase 1E (PPM1E): localization and truncation in brain tissue and effects on neuronal morphology in primary neuronal culture [Ph.D. thesis]*, Georg August University of Göttingen, Faculty of Biology, Göttingen, Germany, 2010, *Dissertation in partial fulfillment of the requirements for the degree "Doctor rerum naturalium"*, http://ediss.uni-goettingen.de/handle/11858/00-1735-0000-0006-ADD4-0.

[21] T. Sawasaki, Y. Hasegawa, R. Morishita, M. Seki, K. Shinozaki, and Y. Endo, "Genome-scale, biochemical annotation method based on the wheat germ cell-free protein synthesis system," *Phytochemistry*, vol. 65, no. 11, pp. 1549–1555, 2004.

[22] H. Takahashi, A. Nozawa, M. Seki, K. Shinozaki, Y. Endo, and T. Sawasaki, "A simple and high-sensitivity method for analysis of ubiquitination and polyubiquitination based on wheat cell-free protein synthesis," *BMC Plant Biology*, vol. 9, Article ID 39, 2009.

[23] Y. Hashimoto, B. A. Perrino, and T. R. Soderling, "Identification of an autoinhibitory domain in calcineurin," *Journal of Biological Chemistry*, vol. 265, no. 4, pp. 1924–1927, 1990.

[24] C. Sinclair, C. Borchers, C. Parker, K. Tomer, H. Charbonneau, and S. Rossie, "The tetratricopeptide repeat domain and a C-terminal region control the activity of Ser/Thr protein phosphatase 5," *Journal of Biological Chemistry*, vol. 274, no. 33, pp. 23666–23672, 1999.

[25] H. Y. Wu, K. Tomizawa, Y. Oda et al., "Critical role of calpain-mediated cleavage of calcineurin in excitotoxic neurodegeneration," *Journal of Biological Chemistry*, vol. 279, no. 6, pp. 4929–4940, 2004.

[26] N. Sueyoshi, T. Nimura, A. Ishida et al., "Ca^{2+}/calmodulin-dependent protein kinase phosphatase (CaMKP) is indispensable for normal embryogenesis in zebrafish, Danio rerio," *Archives of Biochemistry and Biophysics*, vol. 488, no. 1, pp. 48–59, 2009.

[27] M. W. Pinkse, M. Merkx, and B. A. Averill, "Fluoride inhibition of bovine spleen purple acid phosphatase: characterization of a ternary enzyme-phosphate-fluoride complex as a model for the active enzyme-substrate-hydroxide complex," *Biochemistry*, vol. 38, no. 31, pp. 9926–9936, 1999.

[28] D. Barford, A. K. Das, and M. Egloff, "The structure and mechanism of protein phosphatases: insights into catalysis and regulation," *Annual Review of Biophysics and Biomolecular Structure*, vol. 27, pp. 133–164, 1998.

[29] C. C. Chung, P. A. Kanetsky, Z. Wang et al., "Meta-analysis identifies four new loci associated with testicular germ cell tumor," *Nature Genetics*, vol. 45, no. 6, pp. 680–685, 2013.

[30] O. A. Andreassen, W. K. Thompson, A. J. Schork et al., "Improved detection of common variants associated with schizophrenia and bipolar disorder using pleiotropy-informed conditional false discovery rate," *PLoS Genetics*, vol. 9, no. 4, Article ID e1003455, 2013.

Journal of proteome research

Perspective

pubs.acs.org/jpr

Integrated View of the Human Chromosome X-centric Proteome Project

Tadashi Yamamoto,*,† Keiichi Nakayama,‡ Hisashi Hirano,§ Takeshi Tomonaga,∥ Yasushi Ishihama,⊥ Tetsushi Yamada,# Tadashi Kondo,# Yoshio Kodera,□ Yuichi Sato,□ Norie Araki,¶ Hiroshi Mamitsuka,○ and Naoki Goshima●

†Institute of Nephrology, Graduate School of Medical and Dental Sciences, Niigata, Japan

‡Medical Institute of Bioregulation, Kyushu University, Kyushu, Japan

§Graduate School of Nanobioscience, Yokohama City University, Yokohama, Japan

∥Laboratory of Proteome Research, National Institute of Biomedical Innovation, Ibaraki, Japan

⊥Graduate School of Pharmaceutical Sciences, Kyoto University, Kyoto, Japan

#National Cancer Center Research Institute, Tokyo, Japan

□Kitasato University, Kanagawa, Japan

¶Graduate School of Medical Sciences, Kumamoto University, Kumamoto, Japan

○Bioinformatics Center, Institute for Chemical Research, Kyoto University, Uji, Japan

●National Institute of Advanced Industrial Science and Technology (AIST), Tokyo, Japan

ABSTRACT: This article introduces how the human chromosome X-centric proteome project is carried out by the Japan Chromosome X Project Consortium. The inactivation of one of two chromosomes in female mammals and accumulation of genes related to neural/immune systems/tumor/testis are characteristic of chromosome X. In this Chromosome X Project, information on proteins translated from genes on chromosome X is collected by both mass spectrometry- and antibody-based proteomics. Information on the following resources is also provided: antibodies to proteins translated and full-length cDNAs transcripted from the chromosome X genes for recombinant proteins. The consortium aims to provide the following tools to search useful antibodies in the literature (Antibody Ranker), to find gene expression sites in microarray databases (Transcript Localizer) and to do advanced MRM analysis (information-based MRM).

KEYWORDS: *chromosome X, mass spectrometry, antibody, MRM*

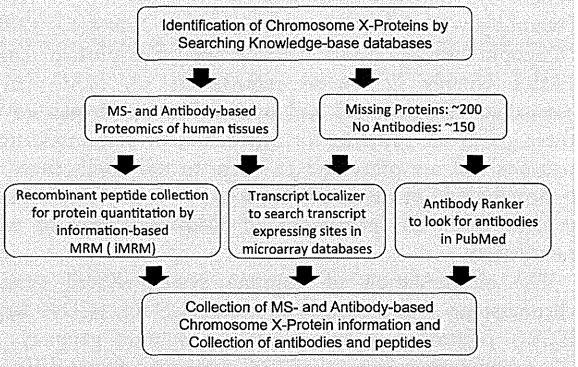

■ INTRODUCTION

Chromosome X is one of the two sex-determining chromosomes (the other is the Y chromosome) in many animal species, including mammals, and is found in both males and females. This chromosome has the following characteristics, which are not found in other chromosomes: presence of sex-determining genes such as androgen receptor gene, inactivation of one of two chromosomes (X-inactivation), a large number of genes associated with human hereditary diseases, and significant accumulation of genes for networks in neuronal, immune and tumor-related systems.

The Japanese Proteomics Society (JHUPO) was chosen to participate in the Chromosome-centric Human Proteome Project and was asked to be in charge of chromosome X. The Japan Chromosome X Project Consortium (JCXPC) was organized to complete the project by collecting information and resources of all proteins translated from genes located on chromosome X (chromosome X-proteins). Knowledge of the human chromosome X-proteins and the current activities and aims of the chromosome X project are briefly described.

■ KNOWLEDGE OF HUMAN CHROMOSOME X

1. Characteristics

The human chromosome X spans about 153 million base pairs (4.94%) out of 3100 million base pairs of total human DNA length. The number of genes on chromosome X is presumed to be 888 genes (4.37%) out of total human genes of 20300.[1] The other sex-determining chromosome, Y chromosome, has only 68 genes and one of these genes, named SRY (Sex-determining

Special Issue: Chromosome-centric Human Proteome Project

Received: September 5, 2012
Published: December 21, 2012

Table 1. Summary of Genes and Proteins on Human Chromosome X

identification level	database	identified/total	%	URL
Transcript	neXtProt	823/874	94.2%	http://www.nextprot.org
neXtProt	neXtProt	615/874	70.4%	http://www.proteinatlas.org/
	Peptide Atlas	396/874	45.3%	http://www.peptideatlas.org
	SRM Atlas	~19000/ ~20300	93.6%[a]	http://www.srmatlas.org
	GPM DB	657/862	76.2%	http://www.thegpm.org
Protein by Antibody	HPA	495/841	55.7%	http://www.proteinatlas.org
	Antibodypedia	722/874	82.6%	http://www.antibodypedia.com
Disorders associated[b]	neXtProt	195/874	22.3%	
	OMIM Gene Map	305/874	34.9%	http://omim.org/geneMap
	Genetics Home Reference	107/874	12.2%	http://ghr.nlm.nih.gov/chromosome/X/show/Conditions

[a]Estimated based on all genes. [b]Including Dominant X-linked diseases (related gene): Vitamin D resistant rickets (X-linked hypophosphatemia, PHEX), Rett syndrome (MECP2), Fragile X syndrome (FMR1), Alport syndrome (COL4A5), etc. X-linked recessive inheritance: Color blindness (OPN1MW, OPN1LW), Hemophilia (F8, F9), Duchenne muscular dystrophy (DMD), X-linked agammaglobulinemia (BTK), Fabry disease (GLA), etc.

Region on the Y chromosome), determines male by inducing and developing the testis to produce a male hormone, androgen. On the chromosome X only a few of the 888 genes directly play a role in sex determination. One is the gene encoding androgen receptor on the chromosome X, indicating the importance of chromosome X in males and suggesting a cross-communication between chromosomes X and Y and also the significance of the androgen receptor in females.

Besides the sex-determining genes, genes in the neural system are uniquely clustered on chromosome X: NLGN3 (Neuroligin-3), NLGN4X (Neuroligin-4, X-linked), OPHN1 (Oligophrenin-1), PAK3 (Serine/threonine-protein kinase), FMR1 (fragile X mental retardation 1), MAG (myelin associated glycoprotein) and others. Proteins translated from these genes are essential for interaction or communication of neurons and are presumed to relate to the intelligence.[2] The important role of the X chromosome in brain function is also evident from the prevalence of X-linked forms of mental retardation.

The accumulation of immune system-related genes to chromosome X also attracts attention. CD40L (CD40 ligand), IL2RG (Cytokine receptor common subunit gamma), BTK (Tyrosine-protein kinase), F8 (Coagulation factor VIII), and F9 (Coagulation factor IX) are example of chromosome X genes that are involved in the immune system and coagulation system.[3]

The inactivation of chromosome X is a process by which one of the two copies of chromosome X in females is inactivated. The inactive X chromosome is transcriptionally silenced to form an inactive structure called heterochromatin. The choice of which X chromosome is inactivated is randomly occurring in each cell in mammals. The X-inactivation center on the X chromosome, which is essential to cause X-inactivation, contains four nontranslated RNA genes, Xist, Tsix, Jpx and Ftx, which are involved in X-inactivation.[4,5]

2. Human Chromosome X-Proteins Identified by Mass Spectrometry (MS)

Information of genes on chromosome X and the proteins encoded by the genes has been collected in several databases (Table 1). In the neXtProt database (http://www.nextprot.org), 874 genes are presumed on chromosome X.[1] Among them, 823 (94.2%) genes have been identified at the transcript level and 615 (70.4%) genes have been demonstrated at the protein level by proteomics. In the other proteome databases, Peptide Atlas and GPM DB (Global Proteome Machine database), 45.3 and 75.2%, respectively, of the genes on chromosome X are identified as proteins. However, these data indicate that more than 200 genes on chromosome X are still unclear whether they translate proteins or not. These unclear proteins are further confirmed by MS and immunohistochemistry using antibodies in this project.

3. Proteomes Identified by Antibody-based Methods

Collection and validation of antibodies against human proteins are progressing by Human Protein Atlas project.[6] By using antibodies, localization of 495 (56.6%) chromosome X-proteins has been examined at cellular and subcellular levels in human body.

The Antibodypedia is a Web site providing datasheets of antibodies against human proteins from antibody providers (http://www.antibodypedia.com). In this collection, datasheets of antibodies against 722 (82.6%) chromosome X-proteins are currently shown although these antibodies have not always been well-characterized in the specificity or reactivity to the proteins for immunolocalization. The Chromosome X Project Consortium members will collect significant evidence of the presence or localization of the chromosome X-proteins from the literature or from their own research.

4. Diseases Associated with Chromosome X

A large number of genes (195 in the neXtProt database) in chromosome X have been demonstrated to associate with genetic disorders and hereditary diseases in humans (Table 1). One of the reasons is only one copy of chromosome X is active both in males (XY) and females (XX) (X-inactivation), resulting in prevalence of X-linked hereditary diseases.

It is estimated that about 10% of the genes (99 genes) encoded by the X chromosome are associated with a family of "CT antigen (cancer-testis antigen)" genes, which encode for markers found in both cancer cells as well as in the human testis (MAGE, GAGE, SSX, SPANX or other CT gene families).[7]

THE JAPAN CHROMOSOME X PROJECT

1. Selection of Tissues and Organs

Since preference in expression of chromosome X genes in neural and immune systems and the tissues (neural and immune systems or cancers and testis) has been demonstrated as described above, it is presumed that expression of chromosome X-proteins is also different among organs or tissues. Therefore, expression of chromosome X-proteins were searched in the kidney, brain, ovary and testis in the Human

dx.doi.org/10.1021/pr300844p | J. Proteome Res. 2013, 12, 58−61

Protein Atlas. As shown in Table 2, there was no significant preference in the expression among the organs. Therefore, the

Table 2. Identification of Chromosome X-Proteins in the Human Protein Atlas[a]

		immunohistochemistry	
	antibodies used	strong (%)	weak (%)
Placenta	627	148 (23.6)	490 (78.1)
Kidney	900	149 (16.6)	654 (72.7)
Ovary	1180	160 (13.6)	825 (69.9)
Testis	1032	224 (21.7)	821 (79.6)
Brain	1112	159 (14.3)	776 (69.8)

[a]Placenta, kidney, ovary, testis and brain tissues were examined by immunohistochemistry using antibodies in the Human Protein Atlas (http:www.proteinatlas.org/). Numbers of antibodies used, stained the tissues strongly or more than weakly are shown (%).

Japan chromosome X project consortium preliminarily chose kidney, ovary, and breast as target sample tissues to look for chromosome X-proteins, which had not been well-identified yet because these organs had not been analyzed by other chromosome projects and our project members had already analyzed the proteomes of these organs more or less.

2. Collection of Protein Existence by MS

With informed consent, human kidney, ovary, breast tissues were obtained from patients when these organs or tissues were surgically removed for treatment of cancers. Kidneys were separated into cortex, medulla and glomerulus.[8] More fine structured (proximal tubule, distal tubule, collecting duct, and others) kidney sections were microdissected from kidney sections by laser microdissection system for deeper and more comprehensive MS analysis of kidney nephron parts. Other organs are also considered for such in depth MS analysis.

Members of the Japan Chromosome X Project are interested in MS analysis of cancers[9−12] and biofluids[13,14] for biomarker discovery and understanding of pathophysiology of cancers. Other members are also focusing on analysis of protein modification such as phosphorylation or glycosylation and collect MS evidence of post-translational modifications of chromosome X-proteins in the target organs and others.[15]

Another approach to find possible tissue or organ sites was carried out to develop a search engine ("Transcript Localizer") to look at human microarray databases and to pick up sites where missing or unclear chromosome X genes are detected.

3. Collection of Protein Localization by Antibodies

Cellular localization of proteins, which would first be identified by MS in the target organs, was secondarily searched in the Human Protein Atlas database and the immunohistochemistry images were retrieved to combine to the data obtained by MS-based proteomics. A prototype of the human kidney proteome database has been opened to the public at the Web site of the HUPO Human Kidney and Urine Proteome Project (HKUPP) Initiative (www.hkupp.org/). The members of the chromosome X project also examined localization of MS-identified proteins in the target organs by immunohistochemistry to confirm the Human Protein Atlas data and the MS identification results. Our consortium will collect information on antibodies to the proteins, which are not provided by the Human Protein Atlas project, by searching in the Antibodypedia.

We are also developing an antibody search engine tool that looks for antibodies in open free access articles in the PubMed database and picks up antibodies to human proteins and collects the following information: name of companies providing antibodies and images obtained by the antibodies. Several different antibodies to one human protein were used in the past studies and the search engine collects information of all of these antibodies and will demonstrate antibody information in a rank order of number of articles in which the same antibody was used. This informs us which antibody is mostly used for a human protein in a community of scientists. Therefore, the tool was named "Antibody Ranker". We believe this tool provides valuable information for researchers who are looking for antibodies for human proteins. Efficiency of the Antibody Ranker is also validated by selecting antibodies for immunohistochemistry in the chromosome X project.

4. Resources and Tools Developed from the Chromosome X Project

The Human Gene and Protein Database (HGPD; http://www.HGPD.jp/) launched in 2008 is a unique resource storing 43249 human Gateway entry clones constructed from the open reading frames (ORFs) of full-length human cDNA, which is the largest in the world.[16] Since the set of these clones are used for recombinant human protein synthesis by the wheat germ cell-free protein synthesis system, this resource is named the Human Proteome Expression Resource (HuPEX).[17] The recombinant protein resource has covered more than 85% of human proteins encoded by 20300 genes.

All synthesized proteins (approx. 18000) have been intensively analyzed by MS after trypsinization and MS/MS information of individual peptides from the proteins has been collected as a database for selection of peptides and MRM (multiple reaction monitoring) transitions. This provides us information to select peptides and MS/MS transitions for MRM (information-based MRM, iMRM) and also resources of reference peptides for quantitation of proteins in the target tissues.

■ CONCLUSION

Current status and future plans of the Japan human chromosome X project are summarized in Figure 1 .. Collaboration and cooperation with other chromosome

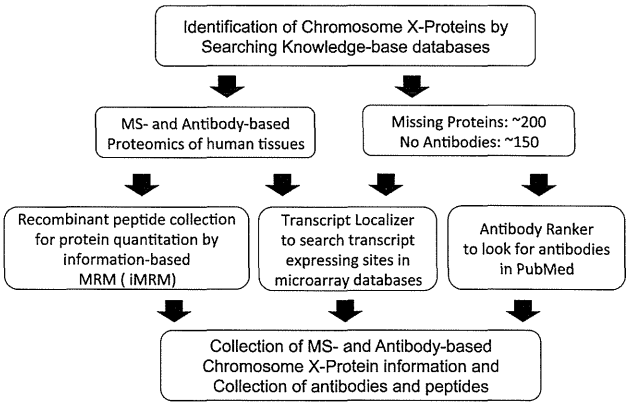

Figure 1. Workflow of Japan Chromosome X Project. Shown here is a strategy from basic collection of knowledge-base proteomics data to final completion of chromosome X proteome data and resource collection done by Japan Chromosome X Project Consortium.

dx.doi.org/10.1021/pr300844p | J. Proteome Res. 2013, 12, 58−61

projects in the Chromosome-centric Human Proteome Project, especially chromosome Y and with other Biology/Disease Human Proteome projects, need to be facilitated to complete the Human Proteome Project.

AUTHOR INFORMATION

Corresponding Author

*E-mail: tdsymmt@med.niigata-u.ac.jp. Tel: +81-25-227-2151. Fax: +81-25-227-0768.

Notes

The authors declare no competing financial interest.

ACKNOWLEDGMENTS

This study was supported by a Grant-in-Aid for Scientific Research (B) to T.Y. ((21390262) from Japan Society for Promotion of Science and by a Grant-in-Aid for Strategic Research Project to T.Y. (500460) from Ministry of Education, Culture, Sports, Science and Technology, Japan and by a Grant-in-Aid for Diabetic Nephropathy and Nephrosclerosis Research from the Ministry of Health, Labor and Welfare of Japan.

REFERENCES

(1) Lane, L.; Argoud-Puy, G.; Britan, A.; Cusin, I.; Duek, P. D; Evalet, O.; Gateau, A.; Gaudet, P.; Gleizes, A.; Masselot, A.; Zwahlen, C.; Bairoch, A. neXtProt: a knowledge platform for human proteins. *Nucleic Acids Res.* **2011**, *40*, D76−83.

(2) Nguyen, D. K; Disteche, C. M. High expression of the mammalian X chromosome in brain. *Brain Res.* **2006**, *1126*, 46−9.

(3) Libert, C.; Dejager, L.; Pinheiro, I. The X chromosome in immune functions: when a chromosome makes the difference. *Nat. Rev. Immunol.* **2010**, *10*, 594−604.

(4) Brockdorff, N. Chromosome silencing mechanisms in X-chromosome inactivation: unknown unknowns. *Development* **2011**, *138*, 5057−65.

(5) Reinius, B.; Shi, C.; Hengshuo, L.; Sandhu, K. S; Radomska, K. J; et al. Female-biased expression of long non-coding RNAs in domains that escape X-inactivation in mouse. *BMC Genomics* **2010**, *11*, 614.

(6) Uhlen, M.; Oksvold, P.; Fagerberg, L.; Lundberg, E.; Jonasson, K.; Forsberg, M.; Zwahlen, M.; Kampf, C.; Wester, K.; Hober, S.; Wernerus, H.; Björling, L.; Ponten, F. Towards a knowledge-based Human Protein Atlas. *Nat. Biotechnol.* **2010**, *28*, 1248−50.

(7) Ross, M.; Grafham, D. V; Coffey, A. J; Scherer, S.; McLay, K.; et al. The DNA sequence of the human X chromosome. *Nature* **2005**, *434*, 325−37.

(8) Miyamoto, M.; Yoshida, Y.; Taguchi, I.; Nagasaka, Y.; Tasaki, M.; et al. In-depth proteomic profiling of the normal human kidney glomerulus using two-dimensional protein prefractionation in combination with liquid chromatography-tandem mass spectrometry. *J Proteome Res.* **2007**, *6*, 3680−90.

(9) Masuishi, Y.; Arakawa, N.; Kawasaki, H.; Miyagi, E.; Hirahara, F.; Hirano, H.. Wild-type p53 enhances annexin IV gene expression in ovarian clear cell adenocarcinoma. *FEBS J.* **2011**, *27*, 1470−83.

(10) Muraoka, S.; Kume, H.; Watanabe, S.; Adachi, J.; Kuwano, M.; et al. Strategy for SRM-based verification of biomarker candidates discovered by iTRAQ method in limited breast cancer tissue samples. *J. Proteome Res.* **2012**, *11*, 4201−10.

(11) Ono, M.; Kamita, M.; Murakoshi, Y.; Matsubara, J.; Honda, K.; et al. Biomarker discovery of pancreatic and gastrointestinal cancer by 2DICAL: 2-dimensional image-converted analysis of liquid chromatography and mass spectrometry. *Int. J. Proteomics.* **2012**, *2012*, 897412.

(12) Sugihara, Y.; Taniguchi, H.; Kushima, R.; Tsuda, H.; Kubota, D.; et al. Proteomic-based identification of the APC-binding protein EB1 as a candidate of novel tissue biomarker and therapeutic target for colorectal cancer. *J. Proteomics* **2012**, *75*, 5342−55.

(13) Kawashima, Y.; Fukutomi, T.; Tomonaga, T.; Takahashi, H.; Nomura, F.; Maeda, T.; Kodera, Y. High-yield peptide-extraction method for the discovery of subnanomolar biomarkers from small serum samples. *J. Proteome Res.* **2010**, *9*, 1694−705.

(14) Kobayashi, M.; Matsumoto, T.; Ryuge, S.; Yanagita, K.; Nagashio, R.; et al. CAXII Is a sero-diagnostic marker for lung cancer. *PLoS One* **2012**, *7*, e33952.

(15) Imamura, H.; Wakabayashi, M.; Ishihama, Y. Analytical strategies for shotgun phosphoproteomics: status and prospects. *Semin. Cell Dev. Biol.* **2012**, *23*, 836−42.

(16) Goshima, N.; Kawamura, Y.; Fukumoto, A.; Miura, A.; Honma, R.; et al. Human protein factory for converting the transcriptome into an in vitro−expressed proteome. *Nat. Methods* **2008**, *5*, 1011−7.

(17) Maruyama, Y.; Kawamura, Y.; Nishikawa, T.; Isogai, T.; Nomura, N.; Goshima, N. HGPD: Human Gene and Protein Database, 2012 update. *Nucleic Acids Res.* **2012**, *40*, D924−9.

Microbiology and Immunology

Microbiol Immunol 2012; **56**: 245–253
doi:10.1111/j.1348-0421.2012.00434.x

ORIGINAL ARTICLE

Specificity of botulinum protease for human VAMP family proteins

Hideyuki Yamamoto[1], Tomoaki Ida[2], Hiroyasu Tsutsuki[3], Masatoshi Mori[4], Tomoko Matsumoto[5], Tomoko Kohda[1], Masafumi Mukamoto[1], Naoki Goshima[5], Shunji Kozaki[1] and Hideshi Ihara[2]

[1]Department of Veterinary Science, Graduate School of Life and Environmental Sciences, Osaka Prefecture University, Izumisano, Osaka 598-8531, [2]Department of Biological Science, Graduate School of Science, Osaka Prefecture University, Naka-ku, Sakai, Osaka 599-8531, [3]Department of Molecular Infectiology, Graduate School of Medicine, Chiba University, Inohana, Chuo-ku, Chiba 260-8670, [4]Japan Biological Informatics Consortium, Aomi, and [5]Biomedicinal Information Research Center, National Institute of Advanced Industrial Science and Technology, Aomi, Koto-ku, Tokyo 135-0064, Japan

ABSTRACT

The botulinum neurotoxin light chain (BoNT-LC) is a zinc-dependent metalloprotease that cleaves neuronal SNARE proteins such as SNAP-25, VAMP2, and Syntaxin1. This cleavage interferes with the neurotransmitter release of peripheral neurons and results in flaccid paralysis. SNAP, VAMP, and Syntaxin are representative of large families of proteins that mediate most membrane fusion reactions, as well as both neuronal and non-neuronal exocytotic events in eukaryotic cells. Neuron-specific SNARE proteins, which are target substrates of BoNT, have been well studied; however, it is unclear whether other SNARE proteins are also proteolyzed by BoNT. Herein, we define the substrate specificity of BoNT-LC/B, /D, and /F towards recombinant human VAMP family proteins. We demonstrate that LC/B, /D, and /F are able to cleave VAMP1, 2, and 3, but no other VAMP family proteins. Kinetic analysis revealed that all LC have higher affinity and catalytic activity for the non-neuronal SNARE isoform VAMP3 than for the neuronal VAMP1 and 2 isoforms. LC/D in particular exhibited extremely low catalytic activity towards VAMP1 relative to other interactions, which we determined through point mutation analysis to be a result of the Ile present at residue 48 of VAMP1. We also identified the VAMP3 cleavage sites to be at the Gln 59-Phe 60 (LC/B), Lys 42-Leu 43 (LC/D), and Gln 41-Lys 42 (LC/F) peptide bonds, which correspond to those of VAMP1 or 2. Understanding the substrate specificity and kinetic characteristics of BoNT towards human SNARE proteins may aid in the development of novel therapeutic uses for BoNT.

Key words botulinum neurotoxin light chain, proteolysis, substrate specificity, VAMP proteins.

Clostridium botulinum is an anaerobic, Gram-positive, spore forming, rod-shaped organism that produces the most potent protein toxin presently known. There are seven serotypes of BoNT, designated A to G. BoNT inhibit synaptic vesicle fusion and neurotransmitter release at nerve terminals, leading to flaccid paralysis. In particular, BoNT serotypes A, B, E, and F are associated with illness in humans, whereas types C and D are mainly responsible for animal botulism. BoNT are composed of two chains linked by a disulfide bond. The 50-kDa LC

Correspondence
Hideshi Ihara, 1-1 Gakuen-cho, Naka-ku, Sakai, Osaka 599-8531, Japan.
Tel: 81 72 254 9753; fax: 81 72 254 9753; email: ihara@b.s.osakafu-u.ac.jp

Received 2 December 2011; revised 16 January 2012; accepted 18 January 2012.

List of Abbreviations: BoNT, botulinum neurotoxins; CDC, Centers for Disease Control and Prevention; dNTP, deoxynucleotide triphosphate; HC, heavy chain; IPTG, isopropyl-β-D-thiogalactopyranoside; LC, light chain; PMSF, phenylmethylsulfonyl fluoride; PVDF, polyvinylidene difluoride; SNAP-25, synaptosomal-associated protein of 25 kDa; SNARE, soluble *N*-ethylmaleimide-sensitive factor attachment protein receptor; TeNT, tetanus neurotoxin; TGN, trans-Golgi network; Ti-VAMP, tetanus neurotoxin-insensitive VAMP; TNF-α, tumor necrosis factor-α; VAMP, vesicle-associated membrane protein.

has zinc-dependent metalloprotease activity and cleaves one of three proteins, collectively termed SNARE proteins: BoNT/A and /E cleave SNAP-25; BoNT/B, /D, /F, and /G cleave VAMP2; and BoNT/C cleaves both SNAP-25 and Syntaxin1 (1, 2). The 100-kDa heavy chain (HC) mediates the cell binding and translocation of the LC into the cytosol. Whereas BoNT have been classified as a category A bioterror agent by the CDC due to their extreme toxicity and relative ease of production (3), BoNT/A is a therapeutic agent that has been used in both cosmetic procedures and to treat strabismus, blepharospasm, hemifacial spasm, cervical dystonia, glabellar facial lines, and axillary hyperhidrosis (4). BoNT/B has also been recently used as a therapeutic agent (5).

The neuron-specific SNARE proteins SNAP-25, VAMP2, and Syntaxin1 are generally examined when investigating BoNT, as they are known target substrates of these neurotoxins. However, it is now well known that SNAP, VAMP, and Syntaxin comprise large families that include multiple proteins (6, 7). In addition to neuron-specific SNARE proteins, other SNARE proteins mediate most membrane fusion reactions in eukaryotic cells, including those involved in cell growth, membrane repair, cytokinesis, and synaptic transmission (8). However, it remains to be clearly demonstrated whether other SNARE proteins are cleaved by BoNT.

The human VAMP family consists of VAMP1/Synaptobrevin1, VAMP2/Synaptobrevin2, VAMP3/Cellubrevin, VAMP4, VAMP5, VAMP7/Ti-VAMP, VAMP8/Endobrevin, Sec22b, and Ykt6. VAMP1 and VAMP2 are primarily found in the synaptic vesicles of neurons and secretory granules of endocrine and exocrine cells, and function as vesicle-associated SNARE of regulated secretion (9, 10). VAMP3 is ubiquitously expressed and is primarily found in sorting and recycling endosomes (10), where it has been implicated in the secretion of α-granules in platelets (11, 12), the recycling of transferrin receptors to the cell surface (13), and the vesicular trafficking of integrins (14, 15). VAMP4 is predominantly localized to the TGN and participates in transport between the TGN and endosomes (16, 17). VAMP5 is preferentially expressed in skeletal muscle and heart. The expression level of VAMP5 has additionally been found to be enhanced during *in vitro* myogenesis of C2C12 cells (18). VAMP7 is involved in vesicular transport from endosomes to lysosomes (19), as well as in apical exocytosis in polarized epithelial cells (20, 21). VAMP8 is detected primarily in early as well as in late endosomes (22, 23), and is required in regulated exocytosis in pancreatic acinar cells (24). Finally, Sec22b proteins have been proposed to play a role in vesicular transport between the endoplasmic reticulum and Golgi (25, 26), whereas Ykt6 is expressed at low levels in most cell types in mammals, in which it functions in Golgi- and endosome-related membrane fusion steps (27–29).

In the present report, we focused on the sensitivity of human VAMP family proteins to BoNT-LC. For this purpose, human VAMP family proteins were prepared using a 'human protein factory', which is developed for human proteomics study, and includes the resources and expression technology required for *in vitro* proteome research (30). We examined the interactions of BoNT-LC/B, /D, and /F with human VAMP family proteins, assessed the kinetic characteristics of the respective LC for their substrates, and finally identified the VAMP3 cleavage sites.

MATERIALS AND METHODS

Construction of BoNT-LC and human VAMP family protein expression vectors

cDNAs coding full-length LC/B and /D were generously gifted by the late Dr H. Niemann and were used as a template to generate expression constructs for these proteins. Total genomic DNA from *C. botulinum* serotype F strain Langeland (NCTC 10281) was used as a template for LC/F. DNA encoding LC/B (1–430) (31), /D (1–436) (32), and /F (1–439) (33) were amplified by PCR in 25 μL reaction mixtures (2 ng template DNA, 10 μM of each of the two indicated primers (Table 1), 2 mM of each dNTP, 0.04 U Phusion Hot Start DNA Polymerase (Finnzymes, Vantaa, Finland), and 5× Phusion HF buffer). Reaction mixtures were heated for 30 s at 98°C and then cycled 25 times with denaturation for 10 s at 98°C, annealing for 10 s at 52°C (LC/B), 45°C (LC/D), or 53°C (LC/F), and extension for 1 min at 72°C (5 min in the final cycle). The resulting PCR products were purified using the GenElute PCR Clean-Up Kit (Sigma-Aldrich, St Louis, MO, USA) and cloned into the pENTR/D-TOPO vector by using the directional TOPO cloning system according to the manufacturer's instructions (Invitrogen, Carlsbad, CA, USA). The resulting clones were verified by sequencing. Subcloned products were then transferred from pENTR/D-

Table 1. Primers used for generation of BoNT-LC

Construct	Primer set
LC/B (1–430)	5′-CACCATGCCAGTTACAATAAATA-3′
	5′-TTAAGCCAAATGCTCCT-3′
LC/D (1–436)	5′-CACCATGACATGGCCAGTAAAAGA-3′
	5′-TTATACTTTTGTAAATAAATCTACTAC-3′
LC/F (1–439)	5′-CACCATGCCAGTTGTAATAAATAGTT-3′
	5′-TTACTTTGTACCTTTTCTAGGAATAAC-3′

Table 2. Primers used for site-directed mutagenesis of VAMP1

Construct	Primer set
E42D	5′-CGAGGTGGTGGACATCATACGTGTG-3′
	5′-TCCACTTGTGCCTGGGTTTGCTGTAG-3′
I48M	5′-GCGTGTGAACGTGGACAAGGTC-3′
	5′-ATGATGTCCACCACCTCCTCCACT-3′
S81T	5′-CCAGTGCTGCCAAGCTAAAGAGGAA-3′
	5′-TCTCAAATTGTGATGCTCCTGCCTGC-3′

TOPO into pDEST17 (Invitrogen) expression vectors through a LR-recombination reaction using LR Clonase II Enzyme Mix according to manufacturer's instructions (Invitrogen).

Entry clones encoding full-length human VAMP family proteins were prepared by the method previously reported (30). pCold TF DNA (Takara, Shiga, Japan) that was cut with *Eco*RI and *Sal*I in a multi-cloning site was ligated to the Gateway cassette frame B (Invitrogen). This plasmid, pCold-TF-Gateway, was converted to pCold-TF-Gateway-FLAG by inserting the FLAG cassette into the *Xba*I site. Entry clones were transferred into the pCOLD-TF-Gateway-FLAG expression vector through a LR-recombination reaction as described above.

Site-directed mutagenesis of VAMP1

Site-directed mutagenesis of VAMP1 was carried out using the Phusion Site-Directed Mutagenesis Kit (Finnzymes), following the manufacturer's instructions. The VAMP1 entry clone was used as a template, and the sites of the point mutations were as follows: at residue 42 Glu was replaced with Asp (E42D); at residue 48 Ile was replaced with Met (I48M); and at residue 81 Ser was replaced with Thr (S81T). DNA encoding E42D, I48M, and S81T was amplified using specific primers (Table 2) that had been phosphorylated by T4 polynucleotide kinase (Nippon Gene, Tokyo, Japan) in 25 μL reaction mixture (100 μM primer, 5× kinase buffer, 10 mM ATP, 0.2 U T4 polynucleotide kinase) for 30 min at 37°C. PCR amplifications were carried out in 25 μL reaction mixtures (2 ng template DNA, 10 μM of each of the phosphorylated primers, 2 mM of each dNTP, 0.04 U Phusion Hot Start DNA Polymerase, 5× Phusion HF buffer) that were preheated for 30 s at 98°C, incubated for 25 cycles of 10 s at 98°C, 10 s at 68°C, and 90 s at 72°C, followed by a 5-min incubation at 72°C. The resulting PCR products were circularized with Quick T4 DNA Ligase (New England Biolabs, Ipswich, MA, USA), purified, and sequenced to confirm the mutations. Recombinant plasmids were transferred into pCOLD-TF-Gateway-FLAG expression vectors as described above.

Expression and purification of BoNT-LC and human VAMP family proteins

Escherichia coli BL21 CodonPlus (DE3)-RIL cells (Stratagene, Santa Clara, CA, USA) were transformed with BoNT-LC expression plasmids and precultured at 37°C overnight in 2 mL LB medium containing 50 μg/mL ampicillin. Cells were then inoculated into 500 mL fresh LB medium containing antibiotics, and grown in a shaking incubator at 37°C until an OD600 of 0.5–0.6 was reached. At this point, culture flasks were allowed to stand on ice for 1 hr prior to the addition of 1 mM IPTG to induce the expression of the recombinant BoNT-LC proteins. Cells were cultured overnight at 16°C before being harvested by centrifugation at 10,000 × *g* for 10 min at 4°C and sonicated in 10 mL ice-cold lysis buffer (20 mM sodium phosphate, 500 mM NaCl, 20 mM imidazole, pH 7.4) containing 1 mM PMSF and 0.1 mg/mL lysozyme. The resulting suspension was centrifuged at 40,000 × *g* for 30 min at 4°C and subsequently passed through a 0.45-μm filter. The filtered lysate was loaded onto a 4-mL Ni Sepharose 6 Fast Flow column (GE Healthcare, Little Chalfont, Bucks, UK) equilibrated with 20 mL binding buffer (20 mM sodium phosphate, 500 mM NaCl, 20 mM imidazole, pH 7.4), the column was washed twice with 10 mL binding buffer, and proteins were eluted with 1 mL × 10 elution buffer (20 mM sodium phosphate, 500 mM NaCl, 500 mM imidazole, pH 7.4). Fractions were analyzed by 12% SDS-PAGE and those containing recombinant BoNT-LC were pooled. The pooled fractions were then subjected to gel filtration on a HiLoad 26/60 Superdex 200 prep grade column (2.6 × 60 cm) (GE Healthcare) equilibrated with PBS, and eluted at a flow rate of 2 mL/min while changes in absorbance at 280 nm were monitored. Peak fractions containing LC were identified by SDS-PAGE and pooled before being concentrated by centrifugal ultrafiltration using an Amicon Ultra-15 centrifugal filter device with a molecular mass cut-off of 10 kDa (Millipore, Billerica, MA, USA), and buffer-changed by passing through a PD10 column (GE Healthcare) equilibrated with cleavage buffer (10 mM Tris-HCl, pH 7.6, with 20 mM NaCl). Protein concentrations were determined by SDS-PAGE and Coomassie Blue staining using known concentrations of bovine serum albumin as standards, and final concentrations were adjusted to approximately 5 mg/mL before samples were stored at –80°C.

Plasmids encoding human VAMP family proteins and VAMP1 mutants were transformed into *E. coli* DH5α cells (Takara), which were then precultured overnight at 37°C in 2 mL LB medium containing 50 μg/mL ampicillin. Cells were inoculated into 1 L fresh LB medium containing antibiotics and grown in a shaking incubator at 37°C until an OD600 of 0.4–0.5 was reached. After cooling

in ice for 1 hr, protein expression was induced by the addition of 1 mM IPTG, and cultures were allowed to grow for 24 hrs at 15°C. Harvested cells were sonicated in 10 mL ice-cold lysis buffer (20 mM sodium phosphate, 500 mM NaCl, 20 mM imidazole, pH 7.4) containing 1 mL Bugbuster 10× Protein Extraction Reagent (Merck KGaA, Darmstadt, Germany), 1% protease inhibitor cocktail (Nacalai Tesque, Kyoto, Japan) and 0.1 mg/mL lysozyme. The suspension was centrifuged at 40,000 × *g* for 30 min at 4°C and subsequently passed through a 0.45-μm filter. Purification was carried out as previously described, except with a molecular mass cut-off of 50 kDa. Purified proteins were concentrated to approximately 10 mg/mL and stored at –80°C.

Cleavage of VAMP family proteins by BoNT-LC

The catalytic activities of BoNT-LC were assayed as follows: 1 μM recombinant LC was incubated with 5 μM VAMP family proteins for 1 hr at 37°C in reaction mixtures made up to a final volume of 10 μL with cleavage buffer. Reactions were stopped by adding 2 × SDS-PAGE sample buffer, and products were resolved by 12% SDS-PAGE. Proteins were detected by Coomassie Blue staining and their expression levels quantified by determining the densitometry of the protein bands using Multi Gauge version 3.0 (Fujifilm, Tokyo, Japan).

Protease activity assays of BoNT-LC for VAMP1, 2, 3, and VAMP1 mutants

VAMP1, 2, 3, or VAMP1 mutants (5 μM) were incubated with several concentrations of LC/B, /D, and /F in cleavage buffer for 10 min at 37°C. Reactions were analyzed by SDS-PAGE as described above. Linear velocity reactions were carried out in 10 μL volumes, and the activity of the reaction was evaluated for 10% cleavage of substrates.

The *Km* and *Kcat* for LC/B, /D, and /F were determined in a reaction with varying concentrations of substrates (0.6–40 μM) following a 10-min incubation at 37°C. The concentrations of LC were adjusted as follows. The concentration of LC/B was 62.5 nM for all substrates. The concentration of LC/D was 500 nM for VAMP1, VAMP1 E42D, and VAMP1 S81T, and was 2 nM for VAMP1 I48M, VAMP2, and VAMP3. The concentration of LC/F was 15.6 nM for VAMP1 and VAMP1 mutants, whereas it was 7.8 nM for VAMP2 and VAMP3. The reaction mixture was subjected to 8% SDS-PAGE and analyzed as described above. Reaction velocity versus substrate concentration was fit to Michaelis–Menten kinetics, and kinetic parameters were derived from non-linear regression equations using GraphPad Prism 4 (GraphPad Software, La Jolla, CA, USA).

Identification of BoNT-LC VAMP3 cleavage sites

LC/B, /D, or /F (1 μM) was incubated for 1 hr at 37°C with 5 μM VAMP3 in cleavage buffer made up to a final volume of 15 μL. Reactions were stopped by adding 2× SDS-PAGE sample buffer. The cleavage of the C-terminal fragment of VAMP3 was evaluated by the appearance of a new band at approximately 15 kDa following electrophoresis on an Any kD Mini-PROTEAN TGX precast polyacrylamide gel (Bio-Rad, Hercules, CA, USA), transferred onto a PVDF membrane, and Coomassie Blue staining. The N-terminal amino acid sequence of this peptide was determined by automated Edman degradation (Nippi Research Institute of Biomatrix, Ibaraki, Japan).

RESULTS

Cleavage of VAMP family proteins by BoNT-LC

In order to carry out an exhaustive analysis of the substrate specificity of BoNT/B, /D, and /F, we generated recombinant proteins of all of the full-length VAMP family proteins (Fig. 1a). VAMP family proteins were incubated with LC/B, /D, and /F (VAMP : LC = 5 : 1) for 1 hr at 37°C. The extent of cleavage was determined by densitometry of Coomassie-stained SDS gels and expressed as a percent of cleavage of substrates (Fig. 1b). VAMP2 and 3 were completely cleaved by LC/B, /D, and /F under the experimental conditions, and although VAMP1 was completely cleaved by LC/B and /F, it was only partially cleaved by LC/D (Fig. 1a). LC/B and /F exhibited similar catalytic activities for VAMP1, whereas LC/D showed activity of <40%, even at 1000 nM (Fig. 1b). VAMP4, VAMP5, VAMP7, VAMP8, Sec22b, and Ykt6 were not catalyzed (Fig. 1a).

In a linear velocity assay examining the catalytic activity of LC/B, /D, and /F for VAMP1, LC/B, and /F again exhibited similar activities, whereby LC/B had only 2.7-fold lower catalytic activity for VAMP1 than LC/F (Fig. 2a). In contrast, LC/D showed 102.2-fold lower catalytic activity for VAMP1 than LC/F (Fig. 2a). For VAMP2, LC/D and /F showed similar activities, with /F showing 4.5-fold lower activity than LC/D, whereas LC/B had 74.2-fold lower catalytic activity than LC/D (Fig. 2b). This was also observed when catalytic activity towards VAMP3 was assessed, as LC/D and /F again showed similar reactivity, whereas LC/B had lower catalytic activity (Fig. 2c). LC/B and F were found to have 58.2- and 9.9-fold

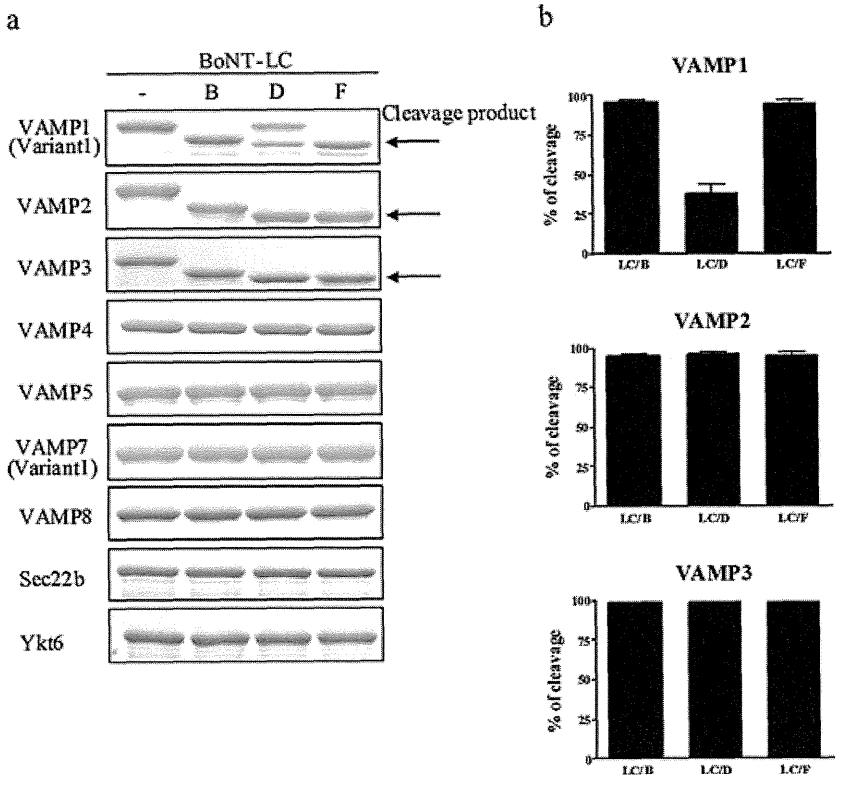

Fig. 1. Catalytic activity of LC/B, /D, and /F. (a) LC/B (1–430), /D (1–436), and /F (1–439) (1 μM) and a control (cleavage buffer) were incubated with the indicated 5 μM full-length human VAMP family members for 1 hr at 37°C. Reaction mixtures were subjected to SDS-PAGE and proteins were detected by Coomassie Blue staining. (b) The amount of cleaved VAMP1, 2, and 3 was determined by densitometry of a Coomassie-stained gel. Standard error bars represent the average of three different experiments.

lower activity towards VAMP3 than LC/D, respectively (Fig. 2c).

Kinetic studies of BoNT-LC cleavage of VAMP1, 2, and 3

Kinetic constants were determined by the cleavage rate of substrates at different concentrations. The derived *Km*, *Kcat*, and *Kcat/Km* values are shown in Table 3. LC/B, /D, and /F had similar *Km* values for VAMP1 and 2, and all exhibited higher affinities for VAMP3. LC/B exhibited similar *Kcat* and *Kcat/Km* values for VAMP1, 2, and 3, whereas LC/D had similar *Kcat* values for VAMP2 and 3, but a 249-fold lower *Kcat* value for VAMP1 in comparison with VAMP2. In addition, LC/D had a 501.6-fold lower *Kcat/Km* value for VAMP1 than VAMP3. LC/F also showed similar *Kcat* values for VAMP2 and 3, and twofold less activity towards VAMP1, relative to VAMP2. Moreover, LC/F had a 2.2-fold lower *Kcat/Km* value for VAMP1 than VAMP3. Although all of the LC exhibited similar trends of affinities for their substrates, their respective catalytic activities were quite different.

Cleavage of VAMP1 mutants by BoNT-LC

As mentioned above, LC/D exhibited a high cleavage efficiency for VAMP2 and VAMP3, and a much lower potency for VAMP1 (Figs 1, 2). In order to determine the residue responsible for the low cleavage efficiency of LC/D towards VAMP1, we compared the sequences of VAMP1, 2, and 3 (Fig. 3). We focused on the three residues in VAMP1 (Glu 42, Ile 48, and Ser 81) that were distinct from VAMP2 and VAMP3 (Asp, Met, and Thr, respectively). VAMP1 mutants were created using site-directed mutagenesis (E42D, I48M, and S81T) and examined for cleavage products. In a linear velocity assay, all three of the LC digested VAMP1 E42D (Fig. 4a) to the same extent as wild-type VAMP1 (Fig. 2a). Interestingly, LC/D, which exhibited only weak activity towards wild-type VAMP1 (Fig. 2a), efficiently digested VAMP1 I48M, with a 1211.3-fold increase in catalytic efficiency. No significant differences in the cleavage of VAMP1 I48M and wild-type VAMP1 by LC/B and /F were observed (Fig. 2a, 4b), suggesting that the I48M mutation influences the substrate cleavage efficiency of only LC/D. LC/B, /D, and /F showed 0.5-, 1.2-, and twofold increases in catalytic efficiencies towards VAMP1 S81T, relative to wild-type VAMP1 (Fig. 2a, 4c).

Studies examining the kinetics of the cleavage of the VAMP1 mutants by LC/B, /D, and /F were also carried out. LC/B, /D, and /F were all found to have similar *Km* and *Kcat* values for the cleavage of the VAMP1 mutants (less than a twofold difference); however, the catalytic activity of LC/D towards the I48M VAMP1 mutant showed a 203.